Loss of PIF7 attenuates shade and elevated temperature responses throughout the lifecycle in Pennycress

Vanessica Jawahir[1], Salma Adam[1], Marcus Griffiths[1], Tad Wesley[2], Win Phippen[2], Nicholas Heller[3], Bhabesh Borphukan[4], Karen Sanguinet[4], and Dmitri A. Nusinow[1†]

[1] Donald Danforth Plant Science Center, Saint Louis, MO 63132, USA

[2] School of Agriculture, Western Illinois University, 1 University Circle, Macomb, IL 61455, USA

[3] Department of Agriculture, Illinois State University, Normal, IL, USA

[4] Department of Crop and Soil Sciences, Washington State University, Pullman, WA 99164, USA

[†]To whom correspondence should be addressed: meter@danforthcenter.org

Abstract

Pennycress (*Thlaspi arvense*) is under development to be grown as a winter annual intermediate oil seed bioenergy crop in the Midwest during typical fallow periods. Crucial work remains to domesticate and optimize pennycress for incorporation into cropping systems and increasing resilience to rising temperatures. We found that increased planting density reduces biomass and swiftens time to flowering and maturity, which are features associated with shade avoidance responses. In controlled conditions, we found that pennycress elongates in response to foliar shade and increased ambient temperatures (20 ˚C to 28 ˚C). We applied the knowledge base from *Arabidopsis thaliana* to manipulate genes in the PHYB signaling pathway to simultaneously decrease the shade avoidance response during interseeding and tissue responses to elevated temperatures. Evaluation of CRISPR alleles of PIF7 shows that *pif7* reduces organ elongation to competition and heat cues and retains a compact rosette when exposed to shade or elevated temperature and their combination. Crucially, yield and oil content were unaltered in *pif7* and plants maintained earlier flowering in stress conditions. Furthermore, indicators of plant health, such as hue, chlorophyll indices, and root system architecture were improved between wild type and *pif7*. This is evidence that plant architecture and physiological health can be uncoupled under competition and heat conditions, supporting our efforts to attenuate morphological responses to environmental cues. We propose this strategy to reduce SAR will improve pennycress performance at high densities, during interseeding establishment in standing crops, and in a warming climate.

Introduction

To sustainably feed and produce biofuels for the rapidly growing human population, agriculture is tasked with increasing production without expanding agricultural land (Ranganathan et al. 2018). The required increases in yield can be achieved by improving crop genetics, increasing planting density, and planting more frequently. Recently, improved yield has come from selecting for tolerance to increased planting densities (Duvick 2005). However, planting densities have to be carefully optimized as excessive density plantings trigger the shade avoidance response (SAR), a syndrome that results from perceived competition for light. SAR, a major limitation to crop planting density, leads to elongated growth, altered tillering, increased lodging, and early flowering, and ultimately results in the underperformance of the shorter species during intercropping (Lu et al. 2023; Li et al. 2021; Tang & Liesche 2017; Liu et al. 2021). Elongation and early flowering are evolutionarily advantageous to increase the fitness of individuals but are undesirable in crop monoculture systems as elongated plants are more prone to lodging, and allocation of resources to these competitive traits often reduces yield (Tang & Liesche 2017; Wille et al. 2017; Raza et al. 2020; Roig-Villanova & Martínez-García 2016; Schmitt et al. 1999).

The effects of SAR have been partially reduced in cereals by breeding for upright leaf angle high in the canopy to better capture light and reduce shading (Wille et al. 2017; Cao et al. 2022). This altered plant architecture has allowed for significant increases in maize planting density from 30,000 plants/hectare to 80,000 plants/hectare, which is a major factor in yield gains (Duvick 2005; Assefa et al. 2018). Improvements in leaf angle have slowed, suggesting this trait is at near peak optimization in maize (Elli et al. 2023) and planting density improvements will need to be accomplished through alternative mechanisms. Leaf angle is not a uniform target for trait improvement in all crops, especially rosette forming crops. An alternative and/or supplemental strategy to altering native architecture is to attenuate SAR and diminish morphological changes that occur in response to high planting density. Studies in Arabidopsis have shown that reduction of SAR reduced shade-induced leaf angle alterations while improving monoculture performance at high densities and increasing weed suppression (Pantazopoulou et al. 2021) supporting that SAR attenuation may be a viable strategy.

The molecular mechanism of SAR has been well studied in Arabidopsis and is a rich resource to mine for candidates for targeted improvement. From the Arabidopsis literature, it is

understood that plants continually monitor the environment for changes in light quality, quantity, and temperature through phytochromes to initiate transcriptional responses to respond to the environmental signals (Oravec & Greenham 2022; Jung et al. 2016). Signaling through phytochromes regulates germination, chlorophyll biosynthesis, photosynthesis, circadian rhythms, shade avoidance, hypocotyl elongation, and flowering times (Kami et al. 2010). Arabidopsis possesses five red/far-red light-absorbing phytochromes (phyA to E) (Sharrock & Quail 1989; Clack et al. 1994; Sharrock 2008). Phytochromes are converted to the Pfr (active) form upon red (R) (660 nm) light exposure and reverted to the Pr (inactive) form either upon far-red (Fr) (730 nm) light exposure, exposure to elevated temperatures, or by incubation in the dark in a process termed dark reversion (Rockwell et al. 2006). PHYB monitors the subtle shifts in R:Fr wavelengths and becomes inactive in low R:Fr. R:Fr in sunlight is approximately 1.15 but is reduced to 0.05- 0.7 in shade as green canopies are effective at reflecting R light but allow Fr to pass through, causing enrichment in the amount of Fr light (Franklin & Whitelam 2005; Smith 1982). A low R:Fr is the cue to an individual that it is being shaded and should initiate SAR to compete with the neighboring plant.

Recently, it was discovered that phytochromes function as thermosensors, due to temperature-dependent PHYB thermal reversion from Pfr to Pr leading to the regulation of plant responses to elevated temperatures (Legris et al. 2016; Jung et al. 2016). Arabidopsis grown in warm temperatures display thermomorphogenic growth by elongating hypocotyls, petioles, roots, alters leaf angle and flowers earlier (Delker et al. 2022; Casal & Balasubramanian 2019; Fernández et al. 2016). Thermomorphogensis and SAR phenotypes are nearly identical in Arabidopsis. This is due to PHYB's shared perception of light quality and temperature and initiation of a common signaling cascade to regulate growth. Combining warm temperatures and shade has been reported to have synergistic effects on Arabidopsis hypocotyl elongation (Burko et al. 2022).

PHYB modulates plant growth through its interaction with PHYTOCHROME INTERACTING FACTORS (PIF) to regulate their post-translational sequestration and turnover (Nozue et al. 2007; Jung et al. 2016; Bauer et al. 2004; Lorrain et al. 2008; Park et al. 2012; Park et al. 2018; Kim et al. 2024). The PIFs induce the expression of auxin biosynthesis genes, leading to organ elongation, which alters plant morphology in response to changing light and temperature conditions (Legris et al. 2019; Pham et al. 2018; Balcerowicz 2020; Li et al. 2012;

Sessa et al. 2018). PhyB in the active Pfr state binds and sequesters PIFs, thereby repressing growth. Growth repression is relieved when the phytochromes are converted to Pr by either far-red light, darkness, or high temperatures, thereby stabilizing the PIFs and inducing elongation programs. Individual PIFs have both distinct and redundant functions to modulate responses in specific environments, allowing for fine tuned growth responses (Pham et al. 2018; Balcerowicz 2020). We hypothesize that the PIFs are prime candidates to target for manipulation to reduce SAR and thermomorphogenesis as they are less likely to result in pleiotropic effects than targeting PHYB- the master regulator.

PIF7 equally participates in the signaling cascade to reprogram developmental responses to both shade and elevated temperatures. In Arabidopsis, *pif7* has reduced hypocotyl elongation in shade, elevated temperatures, and in combination (Burko et al. 2022). In contrast, *Cardamine hirsuta* is shade and heat tolerant and does not elongate its hypocotyl when grown in those environmental conditions. *C. histura*'s blunted elongation response is attributed to reduced PIF7 availability compared to the shade and temperature-sensitive *A. thaliana (Paulišić et al. 2021)*, supporting that modulation of PIF7 activity can confer tolerance to shade and elevated temperature. The reduction in PIF7 shade induced leaf hyponasty, allows *pif7* to more quickly form a dense canopy when grown in monoculture (Pantazopoulou et al. 2021). The dense canopy formed by *pif7* was superior to wild type at suppressing growth of invading plants when grown in field-like conditions (Pantazopoulou et al. 2021).

The literature supports that PIF7 is a key gene modulating growth in shade and temperature. We sought to test if we can simultaneously reduce SAR and thermomorphogenesis by mutating PIF7 in pennycress (*Thlaspi arvense* L.; field pennycress). The pennycress genome is small, diploid, and more than 70% of the predicted peptides of the pennycress genome have more than 80% sequence similarity to those of Arabidopsis (Dorn et al. 2015). Pennycress is in the early stages of domestication as an intermediate oil seed crop with the dual benefit of soil protection during the winter. The September through October planting window is a crucial predictor of yield, therefore in northern US regions, growers will likely need to interseed pennycress into standing crops or in tillage residue, forcing pennycress seedlings to establish themselves under shaded conditions. Pennycress has superior stand establishment when interseeded into soy rather than maize (Mohammed et al. 2020). Superior stand establishment in soybean is attributed to higher light quality and light penetration through its canopy (Mohammed

et al. 2020). Reducing SAR may be key to improving pennycress performance at high density and during interseeding. We hypothesize that reduced SAR in pennycress will allow for higher planting densities to increase yield, provide greater green cover during the winter, and be more tolerant to the fluctuating temperatures in fall and spring. Pennycress is a prime species to test benefits of reducing SAR since overcoming interseeding challenges is relevant to the success of the crop.

In this study, we found that high planting densities negatively impact pennycress biomass and that pennycress is sensitive to shade and elevated temperature. We mutated PIF7 and show that *pif7* has reduced organ elongation when exposed to shade or elevated temperature, and their combination. At high densities, *pif7* has reduced elongation and flowers evenly supporting that reducing SAR is a promising strategy for improving plant performance at high densities.

Results

Planting density affects whole plant morphology and flowering time, but not yield.

Optimizing planting density for any crop is necessary to balance maximal yield potential with competition for nutrients and light. To explore effects of planting density on pennycress morphology and ground cover, *tt8ARV1*, an early commercial pennycress line, was sown in four replicate plots at 3, 5, 7, and 9 lbs per acre in Macomb, IL in 2023. Morphology traits were monitored throughout the 2023-2024 field season. At maturity, five plants from the center of each plot were harvested to characterize morphological differences. Plants at 3 lbs/acre produced the most tillers and had the highest biomass (Figure 1) . Plants sown at 5 lbs/acre developed significantly fewer tillers and had lower biomass. These morphological changes became more pronounced at 7 and 9 lbs/a. Changes in morphology were also apparent at the rosette stage before plants had entered dormancy. 64 days after planting, five rosettes from each plot were harvested and imaged to measure rosette traits and leaf number. PlantCV (v 4.2.1) was used to measure the size and shape of each rosette (Gehan et al. 2017). Rosettes from each planting density had statistically the same leaf area, but became more elongated, determined by a reduced solidity, at 7 and 9 lbs/acre (Supplementary Figure 1). A reduction in solidity typically indicates that a plant is more sparse because the convex hull has a lower percentage of plant material.

Changes in individual plant biomass were significant in both above- and below-ground biomass. Root cores were collected from the center of each plot 179 days post sowing and the number of plants per root core was determined by counting the number of tap roots present in each core. Plots of 5, 7, and 9 lbs/acre had the greatest number of plants per root core, indicating that there were more plants in the higher-density plots. (Supplementary Figure 1). At 3 lbs/a, individual plants had longer total root lengths, larger average root diameter, and more biomass compared to the higher densities (Figure 1 and Supplementary Figure 1). Overall, we have characterized a reduced root and shoot biomass per-plant at higher densities, demonstrating morphological changes secondary to increased planting densities.

Pennycress is a dual-purpose intermediate crop with large rosettes that can protect the soil similar to cover crops. We assessed this secondary benefit of pennycress by determining the percent plant coverage of the total plot area. Drone images of the plots were collected every week starting the February after planting. Percent green coverage was determined by applying a color threshold in each plot to calculate the percentage of the plot covered by plant versus bare soil. The first drone images at day 149 post-sowing are representative of the percent plot protection during the majority of the winter months with minimal above-ground growth during this time. There were no statistical differences in percent green coverage for all planting densities on day 149, and all time points after day 187 post sowing (Supplementary Figure 1). The higher planting densities had greater overall percent green cover during the growth and bolting phase. Green cover plateaued after 200 days post-sowing and began to decrease starting day 235 post-planting as plants began to senesce.

Plots at all densities had an open flower at day 180 post-sowing. Plots sown at 7 and 9 lbs/acre reached 50% and 100% flowering earlier than the 3 lbs/a plots. At maturity, the entire plots were harvested and the average yield from all plot densities were found to be statistically the same. This indicates that increasing pennycress planting density above 3 lbs/a does not increase yield per plot (Figure 1). We hypothesize the morphological responses seen at higher densities reduce per plant yield and are indicative of plant competition within the plot.

Pennycress elongates in response to shade and elevated temperatures.

The reduced tillering and early flowering phenotypes seen at high densities (Figure 1) are classic shade avoidance responses (SAR) and occur in the presence of canopy and neighbor

shade in shade-intolerant plants (Wille et al. 2017; Franklin 2008; Cerdán & Chory 2003). Therefore, we hypothesized that pennycress is shade intolerant and will elicit SAR when planted at high density or when grown in shaded conditions. Pennycress responses to shade were investigated in the MN106 reference background as this line has been bred for laboratory use and is the source of the pennycress genome (Dorn et al. 2015; Nunn et al. 2022). Pennycress seedlings were germinated in white light, then grown under simulated canopy shade by adding supplemental far-red light to reduce the Red:Far red (R:FR) from 2.1 to 0.2 during the day. Seedlings subjected to post-germinative shade had increased hypocotyl elongation, a classic SAR morphological response (Figure 2).

Hypocotyl elongation in shade is observed in shade-intolerant species, such as Arabidopsis (de Wit et al. 2018). The conservation of the photomorphogenic response to shade led us to hypothesize that the red-light signaling pathway likely underlies the SAR phenotypes in pennycress. PHYTOCHROME B (PHYB), the primary photoreceptor responsible for detecting changes in R:FR and initiating or suppressing SAR, is now known to additionally sense temperature. Recent findings demonstrated that elevated temperatures can enhance SAR (Burko et al. 2022; Romero-Montepaone et al. 2020; Casal & Fankhauser 2023). Temperature responses are relevant to pennycress, as winter planting in the upper Midwest is warming most rapidly compared to other seasons (Us Epa 2021). Thus, we included the interaction of shade and temperature to investigate how warm temperatures will affect pennycress planted at various densities. Pennycress growth responses to the moderately elevated temperature of 28 ℃ alone and in combination with shade were measured to investigate their impact on pennycress physiology. Pennycress had more elongated hypocotyls at 28 ℃ and when in combination with shade (Figure 2). Hypocotyls elongated the most in heat alone, while the combination of shade and heat consistently resulted in intermediate elongation compared to individual treatments of shade and heat. Elongation repression with the addition of shade to heat is distinct from that of Arabidopsis (Burko et al. 2022), suggesting that responses to light and temperature are distinct from Arabidopsis.

To determine if elongation in shade and heat extends to other developmental stages, pennycress was exposed to these environmental conditions at the rosette stage. Wild-type pennycress was germinated and grown under control conditions for one week, then maintained under white light or grown under shade, heat, or shade and heat, for an additional week. Shade,

heat, and shade and heat treated plants had increased rosette perimeter (Figure 2) and convex hull area, but lower solidity compared to control conditions (Figure 4), indicating that there is more space between the individual leaves. The altered rosette morphology is attributed to the increased petiole length of leaves when grown under treatment conditions.

Light quality and temperature are critical environmental cues that influence flowering. Earlier flowering is a common phenotype of SAR. When plants are grown at elevated temperatures, progressing to the next generation quickly is a competitive or escape response. Effects of shade and temperature on pennycress flowering time were determined by germinating seeds for 1 week under white light, vernalizing for three weeks, then moving to white light for 4 d before starting shade and/or heat treatment for 14 d. Shade and heat-treated plants bolted earlier than plants grown under control conditions, demonstrating that pennycress alters flowering time in response to environmental cues (Figure 2).

We conclude that pennycress exhibits the classic SAR phenotypes of organ elongation and early flowering indicating that pennycress is a shade avoidant species. Pennycress elongated in response to elevated daytime temperatures, but elongation in heat and shade was not additive. Together, these experiments support that pennycress alters morphology in response to canopy shade and elevated temperatures. The aberrant morphology of pennycress seen at high planting densities may be explained by SAR. We pursued the hypothesis that SAR and thermomorphogenesis are promising candidate responses to target for improvement as a crop.

***pif7* has attenuated responses to foliar shade and heat throughout its lifespan.**

The common morphogenic changes under shade and elevated temperature observed in this study support the hypothesis that light and temperature responses were likely coregulated by PHYB, similar to Arabidopsis (Legris et al. 2016). We reasoned that a pennycress line with altered phytochrome signaling may improve pennycress responses to higher density and temperatures. Morphogenic changes induced by shade and elevated temperature have been modulated by attenuating PIF activity in other species (Fiorucci et al. 2020; Galvão et al. 2019). Mechanistic studies of the shade- and temperature-tolerant *Cardamine hirsuta* demonstrated these responses due to attenuated PIF7 activity (Paulišić et al. 2021). In Arabidopsis, PIF7 is a key regulator of elongation in both shade and at moderately elevated temperatures. Due to reduced SAR by self and neighbor shade, *pif7* plots had quicker canopy closure compared to

wild type and reduced the success of invading plants when grown in field-like conditions (Pantazopoulou et al. 2021), suggesting that reducing SAR could reduce weed emergence in the field. Reduced SAR may also improve the success of intercropping by preventing interspecies competition. The possibility of increasing multiple agronomic traits in wild pennycress compelled us to test if we could manipulate SAR and thermomorphogenic pathways in pennycress by mutating PIF7.

Genomic analysis identified a likely *PIF7* homolog in *Thlaspi arvense,* (TaPIF7). TaPIF7 has 80% nucleotide similarity and over 90% amino acid conservation compared to *Arabidopsis thaliana* PIF7 (AtPIF7) (Supplemental Figure 3). We generated PIF7 mutants in MN106 with CRISPR-Cas9 using 2 guide RNAs to target the second exon and the BHLH domain (Figure 3). Mutated plants were determined by sequencing PIF7 and CRISPR-Cas9 then segregated away to make transgene-free homozygous mutant lines. *pif7-1* is a larger deletion between the two guide RNA sites, deleting 75 amino acids. *pif7-2* had a small deletion of 86 bases starting at the first guide RNA, resulting in a premature stop; the final protein product is predicted to be 122 amino acids instead of 364 amino acids. Due to the severe mutations of *pif7-1* and *pif7-2*, we hypothesize these are knockout alleles. The CRISPR-Cas9 *pif7* alleles had reduced hypocotyl elongation in shade, heat, and shade and heat combined, compared to wild type (Figure 3).

To investigate if mutating PIF7 will have similar impacts in diverse germplasm, we mutated PIF7 in other pennycress genetic backgrounds. Spring32, a wild-type spring ecotype line, and *tt8-t*/ARV1, an early-generation winter ecotype commercial line, were transformed with the CRISPR-Cas9 constructs to target PIF7. We generated additional alleles of *pif7* in each genetic background (Figure 3B and Supplemental 3). Strikingly, the *pif7-1* allele was also obtained in both Spring32 and *tt8-t*ARV1. $pif7_{S32}$ and $pif7_{ARV1}$ mutants have reduced hypocotyl elongation in heat when compared to their parental line (Figure 3 and Supplemental 3), supporting that a PIF7 knockout phenotype is not unique to the MN106 background and could be introduced into elite breeding lines to alter SAR and thermomorphogenic responses.

We further characterized the *pif7-1* in the MN106 background to determine if *pif7* had attenuated SAR and thermomorphogenesis across developmental stages, tissues, and flowering time. Rosette morphology was compared between wild type and *pif7-1* in shade, elevated temperature, and combined conditions for 14 days. *pif7-1* was similar to wild-type under control conditions, remaining compact as indicated by a high solidity, reflecting that *pif7* does not

strongly impact elongation in control conditions (Figure 4). When exposed to shade, heat, and the combined conditions, wild-type plants have a larger rosette convex hull area and a reduced solidity (Figure 4), indicating an elongation response. In comparison, *pif7* had reduced convex hull area and increased solidity when compared to wild type (Figure 4). Petiole length of each leaf was measured after dissecting rosettes. Petioles of *pif7-1* are consistently shorter compared to wild type (Figure 4 and Supplemental Figure 4) even in control conditions. The elongation effect is most prominent in the oldest true leaves as they have been exposed to the environmental stress the longest. The reduced petiole length of each *pif7* leaf results in an overall more compact plant in shade and elevated temperatures.

We sought to holistically characterize the impact of *pif7* on plant growth and responses to the environment. Shade and temperature also affect root development, as sensitive plants allocate more resources to above-ground growth (Salisbury et al. 2007; Rosado et al. 2022; van Gelderen et al. 2018; Gray & Brady 2016). Therefore, the root system was analyzed in each treatment. Total root length remained comparable for wild-type plants grown in all conditions, while *pif7-1* had increased total root length in shade, heat, and combined conditions (Figure 4).

Chlorophyll fluorescence indices are indicative of physiological health and stress levels *(Arief et al. 2023; Ghosh et al. 2023; Murchie & Lawson 2013; Stamford et al. 2023)* and were used to assess if elongation correlates with plant health in shade, heat, and combined conditions, for wild type and *pif7-1*. We measured normalized difference vegetation index (NDVI), chlorophyll index-red edge (CIRE), maximum efficiency of photosystem II (F_v/F_m), and non-photochemical quenching (NPQ), in wild type and *pif7* grown under shade and heat conditions. Wild type had reduced chlorophyll content in shade and heat conditions, as both NDVI and CIRE were significantly reduced, conveying that these environments have a negative effect on chlorophyll content (Figure 4). Both NDVI and CIRE measurements were higher in *pif7-1* than wild type in the same environmental condition, indicating that *pif7-1* is less sensitive to environmental influences on chlorophyll content (Figure 4).

The average F_v/F_m of wild type and *pif7-1* in all conditions is within the typical range expected of healthy plants (Supplemental Figure 5) (Murchie & Lawson 2013). NPQ increased in shade and heat conditions, suggesting that plants are activating protective mechanisms to prevent damage of ROS and was comparable between genotypes (Supplemental Figure 5).

To determine effects of *pif7* on pennycress morphology and life cycle flowering time and inflorescence architecture, wild type and *pif7-1* were grown for 1 week, vernalized to permit the transition to flowering, and then transferred to treatment conditions. Plants were grown under the various environmental conditions for 14 d before returning to control conditions and allowed to mature. *pif7-1* began bolting early under shade, heat, and in combined conditions, but was delayed compared to wild type by 1-2 days in all conditions, indicating that *pif7* has only mild effects on flowering time (Figure 5). At maturity, height was measured to determine if the elongation and early bolting affected overall plant height. Wild type plants were taller in shade, heat, and combined conditions than when in control conditions for their entire life span. Mature *pif7-1* plants grown in experimental conditions were also taller than *pif7-1* plants grown in control conditions, but remained over 10% shorter than wild-type in the comparative condition (Figure 5). This indicates that a short period of shade and warm temperatures have a lasting impact on plant architecture, and that *pif7* can attenuate the physiological impacts of the environment.

***pif7* does not reduce seed oil content, yield, or freezing tolerance.**

Plants were allowed to senesce to collect yield and oil content data. Seeds were harvested from individual wild-type and *pif7-1* plants grown in all conditions. *pif7-1* did not alter total yield or thousand seed weight (TGW) of plants when transiently treated for 14 d during vegetative growth (Supplementary Figure 6). Seed oil content on a dry weight basis (DWB) was also not altered in *pif7-1*. This indicates that mutations in PIF7 do not negatively affect yield or oil content (Supplemental Figure 6).

In Arabidopsis, PIF7 is known to have additional roles in abiotic stress and is a known negative-regulator of DRE-Binding1, a transcription factor important for low-temperature responses (Kidokoro et al. 2009; Lee & Thomashow 2012). PIF7 repression of DREB1 is hypothesized to reduce expression of cold tolerance genes in unstressed conditions and prevent DREB induced growth reduction. We tested cold and freezing tolerance, as it is crucial for pennycress winter survival as an intermediate crop. *pif7-1* survived freezing challenges similarly to wild type (Supplementary Figure 7), suggesting that loss of PIF7 did not greatly affect cold tolerance up to –10 ˚C.

***pif7* has reduced elongation in low light**

If intercropped, pennycress will experience low light and shaded conditions as ground level light intensity (fluence rate) and quality (R:Fr) are both reduced in standing corn and dried soybeans (Supplemental Figure 2). In standing corn, light intensity was reduced nearly 10-fold from approximately 1000 µmol m^{-2} s^{-1} down to 100 µmol m^{-2} s^{-1}. In standing green corn, the R:Fr also significantly reduced to 0.6 at ground level (from 1.4). The reduction in light intensity and quality are a significant hurdle for pennycress to overcome during establishment. Field conditions during sowing were evaluated for effects on yield by comparing plots sown in tilled fields, non-tilled fields, and in standing corn. Pennycress performed poorly when intercropped and had reduced yield when compared to plants sown in open field conditions (Supplemental Figure 2). Pennycress yielded around 500 lbs/ac in both 2019 and 2020, which is significantly less than the expected 1000 lbs/ac or more. Significant yield was lost in 2020 due to late season weather. The yield loss was most pronounced in the tilled and no till conditions. This data, along with our shade studies and morphology data from high density plantings, led us to hypothesize that SAR contributes to the poor interseeding performance of pennycress. Unique to interseeding in standing green corn is the combined pressure of low light intensity and a lowered R:Fr. We sought to explore any effects of low light intensity on pennycress in a controlled environment.

Elongation of wild type and *pif7* was measured in both seedlings and rosettes when exposed to low light. Hypocotyl elongation in response to a titration of light intensity was measured for wild type and *pif7*. *pif7* mutants elongated hypocotyls less in response to reduced light intensity at 20 µmol m^{-2} s^{-1} to 45 µmol m^{-2} s^{-1} (**Figure 5)**. The reduced elongation in low light was not allele specific, as both *pif7-2* and *pif7-1* had statistically similar elongation at 45 µmol m^{-2} s^{-1}.

Elongation in low light was also assessed at the rosette stage. Wild type and *pif7-1* were grown under the recommended control light intensity, 300 µmol m^{-2} s^{-1}, and low light, 80 µmol m^{-2} s^{-1}. Wild type petioles elongate in response to reduced light intensity, while *pif7-1* petiole length is less than wild type when grown in low light.

***pif7* has reduced elongation at high density without impacting yield**

To assess if reducing SAR enhances pennycress performance at high densities, *pif7-1* was sown in mini-fields at seeding rates of 5 and 10 lbs per acre and monitored through senescence.

The mini-fields were vernalized at 4 °C for 3 weeks following a two week germination and establishment period to allow flowering. After vernalization, the mini-fields were returned to the greenhouse and imaged every five days to monitor ground cover and flowering time. As expected, mini-fields sown at 10 lbs/a had a higher ground cover percentage than 5 lbs/a. All genotypes and planting densities reached around 90% green coverage comparable at 15 d post-vernalization (Figure 7).

Density and genotypic effects on individual plant morphology were assessed in 5 individuals harvested at 11 days post-vernalization. This time point was chosen to capture rosette morphology when mini-fields had high green cover, ensuring neighboring plants were touching, but before plants transitioned from vegetative growth to reproduction. Wild-type rosettes at 10 lbs/a had increased convex hull area and perimeter compared to 5 lbs/a (Figure 7). The reduced solidity in wild type at 10 lbs/a compared to 5 lbs/a reflected increased elongation at high planting density. *pif7-1* rosettes maintained their rosette shape at both planting densities, as convex hull area, solidity, and perimeter are not statistically different between 5 lbs/a and 10 lbs/a (Figure 7).

All mini-fields had open flowers at 30 d post-vernalization with wild type at 10 lbs/a averaging the most inflorescences with open flowers. All mini fields reached 100% flowering at 40 d post-vernalization, but had high variability in the number of inflorescences (Figure 7). *pif7* mini-fields looked overall healthier than wild type at both planting densities and flowered more evenly. The center of each wild type mini-field yellowed and failed to flower at both planting densities; plants along the perimeter were the only ones that flowered. *pif7-1* had overall less yellowing and clearings. Yield remained statistically the same for wild type and *pif7-1* at all planting densities despite the unhealthy leaves and the reduced number of flowering individuals in wild type mini-fields.

Discussion

Here we show that mutating PIF7 reduced SAR and thermomorphogenesis in pennycress with limited impacts on plant health, yield and seed oil content. Reducing SAR is a rapid and promising strategy to increase crop performance at high density plantings in diverse environments. *pif7* grown in high density monocultures elongated less and flowered more evenly

than wild type, demonstrating reduced plasticity to the surrounding environment. This reduced plasticity will enable uniform plant growth across millions of acres even while facing various environmental challenges within different hardiness zones. Increasing planting density has been one of the most effective strategies to increase yield. As leaf angle optimizations have slowed (Elli et al. 2023), planting density improvements will need to be accomplished through alternative mechanisms. Superior vegetative architecture varies greatly between species, and will require unique identification and optimization of genetic influences of each specific trait. Alternatively, reducing the capability of plants to change their architecture in response to high density plantings is a more broadly applicable strategy. Coupling superior architecture with reduced responses to neighbor competition could be paramount to maximize plant performance at high densities. This study demonstrates the viability of attenuating SAR to control plant architecture and physiological traits.

Pennycress is currently in the early stages of domestication and presents an opportunity to create a variety suited for use across the US agriculture zones. Widespread adoption of pennycress could produce enough material to convert to fuel to meet the 35 billion gallons of sustainable aviation fuel mandate. Pennycress oil has a fatty acid composition well-suited for conversion to biodiesel and biojet fuel, meets the U.S. Renewable Fuels Standard (Fan et al. 2013), and can produce 600 liters ha^{-1} (65 gal ac^{-1}) of oil annually without competing for land use with food crops (Moser et al. 2016; Moser 2012). This, combined with ecosystem services provided by growth over the winter when fields typically lay fallow, positions pennycress as a strong candidate crop to meet our future mandated sustainable aviation fuel goals (Fan et al. 2013; Griffiths et al. 2022).

Pennycress responds to high density plantings and environmental cues

Here, we have shown that both above- and below-ground biomass was negatively impacted by high density plantings in the early commercial line *tt8ARV1* and did not increase yield (Figure 1 and Supplemental Figure 1). Overall, this data supports the conclusion that pennycress has high phenotypic plasticity and acutely responds to the environment.

Our study finds that pennycress is shade and heat intolerant and responds to simulated canopy shade by elongating hypocotyls and petioles and flowering earlier. Elongated petioles at the rosette stages increase rosette perimeter and convex hull area, and expose more soil between

the leaves(Figures 2, 4). Etiolated plants reduce robust stand establishment and will reduce soil coverage in the field, thereby decreasing ecosystem benefits of weed suppression and soil preservation (Griffiths et al. 2022; Pantazopoulou et al. 2021). The elongation phenotypes in our controlled environments are similar to the phenotypes we observed in high density field plots, suggesting that pennycress SAR reduces per plant performance with increasing density.

Light quality and quantity are both reduced at ground level in fields with a standing crop, which may reduce pennycress stand establishment when intercropped (Supplemental Figure 2). Our findings provide critical considerations for growers when making decisions about field conditions at the time of planting. Elongation in response to low light and shade may also limit the ability to intercrop current pennycress varieties into existing corn and soy rotations, particularly in northern states where summer crops are often not harvested before September. While delaying pennycress planting until after corn harvest has consequences for pennycress yield, (Cubins et al. 2019; Dose et al. 2017; Patel et al. 2021; Bishop & Nelson 2019), early planting can be equally challenging as temperatures continue to increase during the fall in the Midwest, (Us Epa 2021) triggering thermomorphogenesis.

Altering pennycress morphology by perturbing PHYB signaling

We sought to simultaneously reduce SAR and thermomorphogenesis by manipulating the PHYB signaling pathway. We targeted PIF7 as it plays dual roles in elongation to shade and temperature in Arabidopsis (Burko et al. 2022; Fiorucci et al. 2020; de Wit et al. 2016; Galvão et al. 2019). Two CRISPR alleles were generated in MN106, Spring32, and *tt8ARVI* backgrounds, lines bred for laboratory usage and the first generation commercial line, respectively. *pif7* alleles in all genetic backgrounds had reduced elongation in heat. CRISPR-Cas9 nuclease was effectively targeted by the two gRNAs that we selected which successfully regenerated an identical allele, *pif7-1*, in all three genetic backgrounds. This feat demonstrates that CRISPR-Cas9 mutagenesis has the capacity to generate identical alleles independently, likely through repair through microhomology regions (Schiml et al. 2016), similarity of the PIF7 sequence, and precise targeting of CRISPR. All *pif7* alleles in the MN106 background had comparably reduced hypocotyl elongation to shade, heat, and shade plus heat. This informs us that the *pif7* alleles have similarly reduced function of PIF7 and are likely complete knock-outs.

The wild-type lines (MN106, Spring32, and *tt8*ARV1) all elongated in heat, but to varying degrees. The variability in elongation response suggests that there is natural phenotypic variability to heat, and yet all PIF7 mutants had the same effect of reducing response (Figure 3 and Supplemental Figure 3). This evidence also supports the hypothesis that PIF7 has a conserved function across accessions and is a viable candidate for manipulation across pennycress genetic backgrounds. In summary, our study implies that PIF7 is part of a shade and elevated temperature signaling cascade affecting plant development.

pif7-1 attenuated petiole elongation, flowering time, and inflorescence stature while better maintaining chlorophyll content compared to wild type in all treatment conditions (Figures 4 & 5). Shade and heat alone, or in combination continued to shorten time to flowering in *pif7-1* compared to wild type in control conditions (Figure 5). The shortening of time for pennycress to flower could be an agronomic benefit to speed up the life cycle and ensure compatibility of the winter crop with planting of summer cash crops. Thus, our results suggest that *pif7* pennycress would be ready to harvest earlier for better complementation for growers to sow their summer crop.

Pennycress holistically responds to the environmental cues by altering root growth. This observation aligns with findings in Arabidopsis literature, where low R:Fr restricts root growth and development (Rosado et al. 2022; van Gelderen et al. 2018). Diversion of critical resources to shoot growth is hypothesized to enhance competitiveness in suboptimal light quality. *pif7* continues to develop roots in shade and elevated temperatures, suggesting that it is not reallocating resources to only promote shoot growth and has dampened the competitive growth reprogramming response (Figure 4). Greater root length enhances plant resource capture of water and nutrients by increasing soil exploration and root-soil contact, thereby improving plant resilience and nutrient catch as a cover crop (York et al. 2013; Griffiths et al. 2022).

Plant health and yield in the absence of SAR

Elongation is thought to provide either a competitive advantage to outgrow shade casting neighbors or protection from hot soil. It is imperative that *pif7* or reducing SAR does not have physiological consequences negatively impacting yield and plant health. This study sought to understand if elongation provided a physiological benefit to plants in our test environments by

measuring chlorophyll indexes that are commonly used to assess plant stress (Murchie & Lawson 2013; Maxwell & Johnson 2000; Arief et al. 2023).

Wild type and *pif7-1* individual plants had F_v/F_m measurements near the idealized 0.8 measurement in control conditions, shade, heat, and shade plus heat, indicating that these conditions are not stressful enough to damage PSII (Supplemental Figure 5). PSII chemistry still maintains the capacity to function at maximum efficiency. This *pif7-1* heat treatment outliers could be due to inadequate dark adaptation which results in lower measurements overall. A lowered F_v/F_m of *pif7* compared to wild type in any condition would be concerning that PIF7 is needed for health or that the elongated phenotype is needed for physiological protection. Our results do not substantiate that concern. This result is substantiated since NPQ increased similarly in the test conditions between wild type and *pif7-1*. NPQ is a protective mechanism that increases when plants experience high light stress or other abiotic stresses (Ghosh et al. 2023; Murchie & Lawson 2013; Stamford et al. 2023). NPQ increased similarly in the test conditions between wild type and *pif7-1*, suggesting that plants are activating protective mechanisms to prevent damage of ROS and this response is preserved in *pif7* (Supplemental Figure 5).

Seed quantity, weight, and oil content were not significantly altered in *pif7* compared to wild type in control and experimental conditions (Supplemental Figure 6). These data support that *pif7* does not have a drag on yield. *pif7* maintained freezing tolerance and requirement for vernalization (Supplemental Figure 7).

Overall, we did not find evidence of growth or photosynthetic impairment in *pif7*, as *pif7-1* remained comparable to wild type when grown in control conditions. We believe *pif7* does not have a negative effect on traits and therefore this mutation is viable for integration into elite breeding lines.

The potential for *pif7* to improve interseeding.

Low light intensity and shade are critical challenges for pennycress establishment in intercropping scenarios (Supplementary Figure 2). When interseeded into standing corn, pennycress will face the complex environment of low fluence and low R:Fr (Supplementary Figure 2). The etiolated morphology that pennycress adopts when grown in standing corn is hypothesized to contribute to poor establishment and reduced yield (Supplemental Figure 2). Reducing elongation in low light and shade may improve interseeding success. Our study

demonstrates that, in controlled low fluence environments, pennycress phenocopies morphology in reduced R:Fr by similarly elongating hypocotyls and petioles (Figure 5). *pif7* had reduced hypocotyl and petiole elongation in low light compared to wild type and was not allele specific. This novel finding implicates the PHYB-PIF signaling hub as a regulator of morphology responses to low light.

The primary mechanism by which plants signal in response to low light is not fully understood. In Arabidopsis, leaf hyponasty is reduced in some of the *pifs*, implicating the PHYB signaling pathway (Trupkin et al. 2014). Contrary to this, Arabidopsis has a delayed rosette vegetative phase that changes in low light and is independent of photoreceptors altogether (Xu et al. 2021). Our data is the first to implicate *pif7* function in low fluence and suggests that canonical red light signaling has a role in growth responses to low fluence.

Potential to increase planting density

Our ultimate goal is to reduce the undesirable morphogenic changes associated with SAR, allowing for plants to maintain ideal architecture when grown at high density. We tested *pif7* performance in a common garden experiment by sowing mini-fields at 5 lbs/a and 10 lbs/a, both densities higher than the recommended 3 lbs/a. This was performed in a temperature controlled greenhouse to specifically test effects from density and reduce confounding variables.

Our mini-field experiments also showed that *pif7* had reduced rosette elongation at 10 lbs/a and is statistically the same as wild type at 10 lbs/a in rosette morphological characteristics (Figure 7). This shows that SAR and light quality do contribute to the elongated phenotypes seen at high density plantings in the field. The *pif7* mini-fields looked healthier than wild type because they had reduced yellowing and flowered uniformly in the mini-fields, yet yield remained statistically the same for both genotypes and planting densities. It appears there is a yield loss at 10 lbs/a but that trend is not statistically captured in this trial with low replication and high variability.

This mini-field experiment demonstrated that *pif7* rosettes remain compact at a high planting density and successfully attenuates elongation and flowering responses associated with SAR at high planting densities. The compact morphology of *pif7* is unlinked to yield, supporting a hypothesis that we can improve vegetative growth responses to the environment without a drag on yield.

Summary

We have used the foundational knowledge from the Arabidopsis red-light signaling pathway to reduce plasticity to environmental cues in pennycress. The creation of a PIF7 mutant, attenuated elongation in shade, elevated temperatures, and at high density plantings. This study supports that reducing SAR is a promising strategy to optimize plants for high planting densities.

Methods

Plant materials

MN106 is the primary wild type line used throughout the paper. Spring32 and *tt8ARV1* are also wild type lines and were used as genetic backgrounds to generate additional PIF7 mutant alleles. *tt8ARV1* is an early commercial line with a mutation in TRANSPARENT TESTA 8. *pif7-1* was generated in MN106, Spring32, and *tt8ARV1* backgrounds. *pif7-2* was generated via CRISPR in the MN106 background. *pif7-4* was generated with CRISPR in the Spring32 background while *pif7-5* was generated in the *tt8ARV1* background. MN106 is the parental background unless otherwise denoted with a subscript. MN106 *pif7-1* is the primary line used to characterize PIF7.

Field trial

The field trial was conducted at Western Illinois University in Macomb, IL, USA (40.4885, -90.6902). The preceding crop was Cereal rye that was harvested June 26th, 2023. 50lb. N (28% UAN)+ 10lbs. Sulfur (Thiosulfate) was applied as a liquid on September 26. Treflan was applied on all plots at a rate of 1 qt./acre and double incorporated with tillage. Seed was prepared into planting packets. Pennycress seed was broadcast on September 29th 2023 with ½ inch water applied within 24 hours of planting. Plots were 4’ x 10’ in size and sowed at 3, 5, 7, and 9 lbs/acre.

5 rosettes were removed from each plot 64 days after planting on December 04, 2023 after plants slowed growth. Rosettes were imaged with an overhead camera to analyze rosette morphology.

On May 15, 2024, at maturity, 5 whole plants from the center of each plot, including the root system, were harvested. All plants were individually imaged. The number of tillers arising from the basal rosette were manually counted. Plants from the same plot were dried down together and weighed as a group to calculate biomass.

One soil core was taken from the middle of each plot and directly over one plant ensuring that the section that was cored represented the whole plot. Soil cores were taken from the field on March 27th, 2024, 179 days post planting using a bulb and garden planter with 6” depth x 3” diameter dimensions. Cores were placed in plastic bags and stored at -20 ℃ until washing. After defrosting in a water bath, the soil cores were carefully washed by hand with the roots cleaned and separated from particulate organic matter. Washed roots were then stored in clean plastic bags at 4 ℃ and were imaged in the following days using an Epson Expression 12000XL flatbed scanner equipped with a transparency unit (Epson America Inc, Los Alamitos, CA, USA). Roots from the soil core were carefully separated in a water filled plastic tray into individual plants by the tap root. Roots were placed on square plates (150 mm × 150 mm) filled with a 10 mm layer of deionized water with one tap root per tray. Unconnected roots from neighboring plants that had no tap root were placed in a separate square plate. All roots were spread-out using forceps to avoid overlap between roots. Six trays were imaged at once with the scanner using the Epson Scan 2 software (Epson America Inc, Los Alamitos, CA, USA) at a resolution of 600 dpi as a JPG file with 99% quality. The individual root images were cropped out the main image and root measures were computed using RhizoVision Explorer v2.0.2 (Seethepalli et al. 2021). In the software, the tap root length, lateral root length, and tertiary root length was classified by root diameter threshold ranges of > 0.4 mm, 0.4 - 2 mm, and < 2 mm, respectively. The image thresholding level was set to 200, and root pruning threshold set to 20 pixels. After scanning, the root material was placed in a paper envelope and dried at 60 ℃. In this way root length density for the plot was determined after aggregating individual plant data together by core. Root length per plant was determined by averaging the root measures by number of tap roots per plot.

Drone Imaging and Analysis

Drone images were taken after the hard frost period throughout the spring to harvest starting on February 27, 2024 and finishing on May 27, 2024. The whole field was imaged every 7 to 10 days with a total of 12 flights. The drone used for data collection was a DJI Mavic 3M

and was equipped with a multispectral sensor camera. Flights were pre-programmed using DJI Pilot 2 and were conducted at 17 m height above the ground with an image resolution of 0.75 cm/pixel. Images were collected at an approximate flight speed of 1.5 m/s. There was 70% side overlap and 80% frontal overlap in the collected images. The time of the day for each flight was around 9 am CDT ensuring the weather conditions were similar. Images were assembled into orthomosaics using WebODM v. 2.5.

Image analysis was conducted on the orthomosaic images using a custom Open-CV python code. A reference scale was established for each orthomosaic using the known field distance and a scaling factor was applied to ensure consistent dimensions across plots. Then the images were rotated ensuring each image had the same orientation. Individual plots were then cropped out as a grid layout and plots names were assigned to the images. To differentiate between bare soil and vegetation, a soil mask was generated using the Blue-Green Index (BGI). Pixels with BGI < 0.15 were classified as soil. Additionally, a green leaf index (GLI) was used to differentiate green and senesced vegetation based on a GLI threshold of 0.2 (>= 0.2 green, < 0.2 senesced). The indices used are defined as:

$BGI = (G - B) / (G + B + \varepsilon)$, $GLI = (2 * G - R - B) / (2 * G + R + B + \varepsilon)$

Where R, G, and B are the red, green, and blue channels of the image, respectively, and ε is a small constant to avoid division by zero. The percentages of green tissue and senesced tissue were calculated relative to the total pixel count within the plot. To ensure accurate cropping and thresholding, a reference image was generated for each plot by overlaying the indices on the original orthomosaic for manual validation.

Interseeding with corn

Fields in a corn-soy rotation were used for this experiment in 2018-2019 and 2019-2020. Black-seeded MN106 pennycress seeds were used in the split-plot experiment in Lexington, IL (40.668868, -88.783464) and Normal, IL (40.519860, -89.010891). The whole plot factor was the management of the corn harvest and stover post-harvest (pennycress interseeded into standing corn before corn harvest, pennycress no-till drilled into corn stover, and pennycress drilled into a prepared seedbed) and the subplot factor was seeding rate (5 lbs/ac and 10 lbs/ac). From the whole plots that were 9.14m wide and 18.29m long, the sub plot was 4.57m wide. Data

were collected from the middle 3.05m of the plot and the middle 15.24m of the length to avoid any impact from the edge of the plot. Seed yield was measured with a Kincaid plot combine.

Seed sterilization and growth conditions

Seeds were sterilized with a 30% bleach and 0.1% triton solution for 15 minutes and washed three times with sterile water. For bulk sterilization, seeds were gas sterilized by arranging seeds in a single layer and exposed to chlorine gas for 5 hrs. Seeds were plated on ½ strength Murashige and Skoog (MS) medium and stratified at 4 °C for 3-5 d. Plates were grown at 130 µmol/m-^{2}/s^{-1} in 12:12 light:dark cycles at 22 °C for 4-7 d then vernalized at 4 °C with 12:12 light:dark for 3 weeks, unless otherwise noted.

Hypocotyl measurements were taken by growing seeds for 2 d at 22 °C 12:12 control conditions then changed to appropriate experimental conditions for the indicated number of days. White light conditions were a 12 hr day/ night at a constant 22 °C. For heat treatment, plates were grown at 28 °C during the day with a 12 hr day/night cycle and 22 °C night temperature. Canopy shade was simulated by adding a far-red light during the day time to reduce the R:Fr to 0.3. A constant temperature of 22 °C was maintained at plant level by reducing the chamber settings to 20 °C during the day to compensate for the heat given off from the far red lights. Temperature readings were collected every 5 min for the entirety of the experiment with a HOBO meter to ensure chambers were at the proper temperature. For the shade + heat treatment, plates were incubated under far red light during the day at a R:Fr of 0.3. A day time temperature of 28 °C was maintained by setting the chamber to 25 °C during the day when the far red lights were on. The night temperature was 22 °C. A HOBO meter was used to monitor temperature.

Plants grown for rosette measurements were sown directly in soil in 3.5 in pots. Light intensity was 200 µmol/m-^{2}/s^{-1} with a 16:8 light/dark cycle at 22 °C. Plants had to have visible true leaves before beginning experimental conditions. A day-time temperature of 28 °C was the heat treatment. Shade was simulated with the addition of far red to reduce the R:Fr to 0.3. Chamber temperature was set to accommodate the heat generated by the far red lights to be 22 °C (shade only) or 28 °C (shade + heat). Night temperature was 22 °C. Rosettes were imaged on the indicated day.

Plant transformation and selection

Plants were transformed using *Agrobacterium tumerfaciens* strain GV3101 by submerging inflorescences in Agro solution and placed in a vacuum under 27 inches of mercury for at least 10 minutes (McGinn et al. 2019). Inflorescences were wrapped with saran wrap and placed in the dark overnight. In the morning, plants were returned to standard growth conditions and allowed to mature.

T_1 seeds were selected by growing on 50µg/mL of hygromycin for 2 weeks. Resistant plants were vernalized and rescued to soil. Plants were genotyped to confirm presence of CRISPR and mutations to the target gene.

Generating CRISPR alleles

Two guide RNAs were designed with Cas-designer (Park et al. 2015) to target the PIF7 coding region. Guide RNAs (gRNA) were cloned into a pHEE401 CRISPR-containing vector as described. The first gRNA with PAM sequence is TCTTGGGCGTCTTTCGAATCTGG. The second gRNA plus PAM sequence is CGATTCACAACGAGTCTGAAAGG. The pHEE401 containing gRNAs and CRISPR was transformed into pennycress lines: MN106, Spring 32, and *tt8ARV1*. T_1s were grown for 14 days on ½ MS agar plates containing 50µg/mL hygromycin for selection. T_1s were genotyped using primers to amplify the region spanning both gRNA targets. PCR product was sent for sequencing to determine presence of mutations. Lines containing desirable mutations were propagated until homozygous for the mutation and the absence of transgenic elements. Tiling PCR was used to confirm the complete absence of CRISPR-CAS9 in the final lines.

Image analysis

Whole seedlings were laid out on an MS agar plate with a ruler in the same plane as the plants. The plate was backlit with a lightboard and imaged with an overheard mounted camera. Hypocotyls were individually measured using ImageJ.

Rosettes were photographed with an overhead mounted camera on the indicated day. A color card was included in every image to serve as a size reference and allow for color correction if necessary. Images were processed with PlantCV (v 4.2.1) by white balancing each image and then thresholding to isolate the plant from the background. The analyze.size function was used to measure shape characteristics and size. The chip size of the color card was measured using the

transform.detect_color_card function. The chip size in pixels was used to convert appropriate results to metric measurements.

Mini-fields were imaged with an overhead mounted camera with a color card in every image. Machine learning was used to train the naive.bayes function of PlantCV to distinguish between plant and background. Only plant and background material within the perimeter of the mini-field box was used to calculate percent ground cover.

Density trial

Holes were drilled into Sterilite 27L boot boxes measuring 59.7 cm L x 42.9 cm W x 14.9 cm H for drainage and each is considered a mini-field. Three independent mini-fields of each planting density and genotype that were arranged at random in the greenhouse. Seeds were broadcast, allowing for random spacing of seeds. The mini-fields were grown for 2 weeks to allow seeds to germinate before vernalizing for 3 weeks. The mini-fields were fertilized once a week in the greenhouse.

Fields were imaged every 5 d after vernalization. Inflorescences were counted using the cell-counter ImageJ plugin to score open and unopened inflorescences. After senescence, the entire mini-field was harvested to calculate total yield per mini-field.

Measuring Chlorophyll Fluorescence

Seeds were sown and grown in long day conditions for 7 d then changed to the appropriate treatment condition and grown for an additional 14 d. Rosettes were imaged with the PhenoVation CropReporter imaging system. Plants were dark adapted for a minimum of 20 minutes before imaging. NPQ, NDVI, and color analysis were taken. Each indice was quantified using the corresponding function in PlantCV.

Freezing trial

MN106 and *pif7-1* were grown under controlled conditions in a growth chamber maintained at 22°C with a 16-hour light/8-hour dark photoperiod. Seedlings were grown for two weeks at 22°C before being transferred to a vernalization chamber set at 4°C with an 8-hour light/16-hour dark photoperiod for three weeks to induce cold acclimation. The experiment was

repeated across five independent batches, each consisting of 12 seedlings per genotype, resulting in a total of 60 seedlings per line for survival evaluation.

Following cold acclimation, seedlings were transferred to a programmable environmental chamber (LU-113, Espec Corp., Hudsonville, MI, USA) for the freezing treatment. Plants were initially held at 4°C for 30 minutes, followed by a gradual temperature reduction at a rate of 2°C per hour until reaching -3°C. This temperature was maintained for 16 hours to promote ice nucleation and pre-freezing conditioning. Subsequently, the temperature was further decreased to -10°C at the same rate (2°C per hour), and plants were held at this target freezing temperature for 2 hours. After freezing, the temperature was gradually increased back to 4°C at 2°C per hour, where plants were held for 1 hour before being returned to standard growth conditions (22°C, 16-hour light/8-hour dark) for recovery.

Plant survival was assessed 1–2 weeks post-treatment, based on visible regrowth and meristem viability. Plants were considered "survived" if new leaf growth emerged and the meristem remained viable. This experimental design enabled comparative assessment of freezing tolerance between MN106 wild-type and *pif7* mutant lines under controlled freezing conditions.

Seed oil content

Total seed oil content and moisture were determined by nondestructive TD-NMR on 450 mg samples of whole pennycress seed using a Bruker MQ40 and Minispec Plus version 7.0.0 software to calculate weight percent oil and moisture. TD-NMR was performed on the samples and standards with a Bruker Minispec MQ40 with a 39.95 MHz NMR frequency and 40°C magnet temperature. The 90° and 180° pulse lengths were 11.48 µs and 22.98 µs respectively. A 23° detection angle, gain of 44 dB, pulse attenuation of 15 dB, recycle delay of 2 s, window 1 of 0.055 ms, window 2 (τε) of 7 ms, and 724 magnetic field steps were set to employ a Hahn spin echo effect for signal collection. Each sample employed 16 scans at a receiver gain of 59. Weight percent oil and moisture calibration curves were constructed within the Bruker software for oil standards (20% - 40% oil) and moisture levels (6% - 11% moisture). For sample analysis, 450 mg of whole pennycress seed into 10 mm flat bottom NMR tubes, tempered at 40°C in a heat block for 30 minutes, and scanned in the MQ40. The Minispec Plus software applied the standard curves and the results were exported to Excel. The percent oil on a dry weight basis was

calculated by dividing the milligrams of oil in each sample by the dry weight of each sample and multiplying by 100.

Funding

This study was supported by the U.S. Department of Energy, Office of Science, Office of Biological and Environmental Research, Genomic Science Program grant no. DE-SC0021286 to Dmitri A. Nusinow.

Author contributions

Vanessica Jawahir and Dmitri Nusinow designed this project. Vanessica Jawahir wrote the manuscript, designed, performed, and analyzed experiments. Salma Adam performed and analyzed experiments. Marcus Griffiths collected and analyzed soil cores, and analyzed drone images and root morphology in field and controlled experiments. Tad Wesley and Win Phippen designed and performed the in-field density experiment and collected drone images throughout the field season. Wesley and Phippen assisted with all field sample collections and analyzed seed oil content. Nicholas Heller designed and performed the interseeding field experiment. Bhabesh Borphukan and Karen Sanguinet designed and performed the freezing tolerance experiment. All authors edited and reviewed the manuscript.

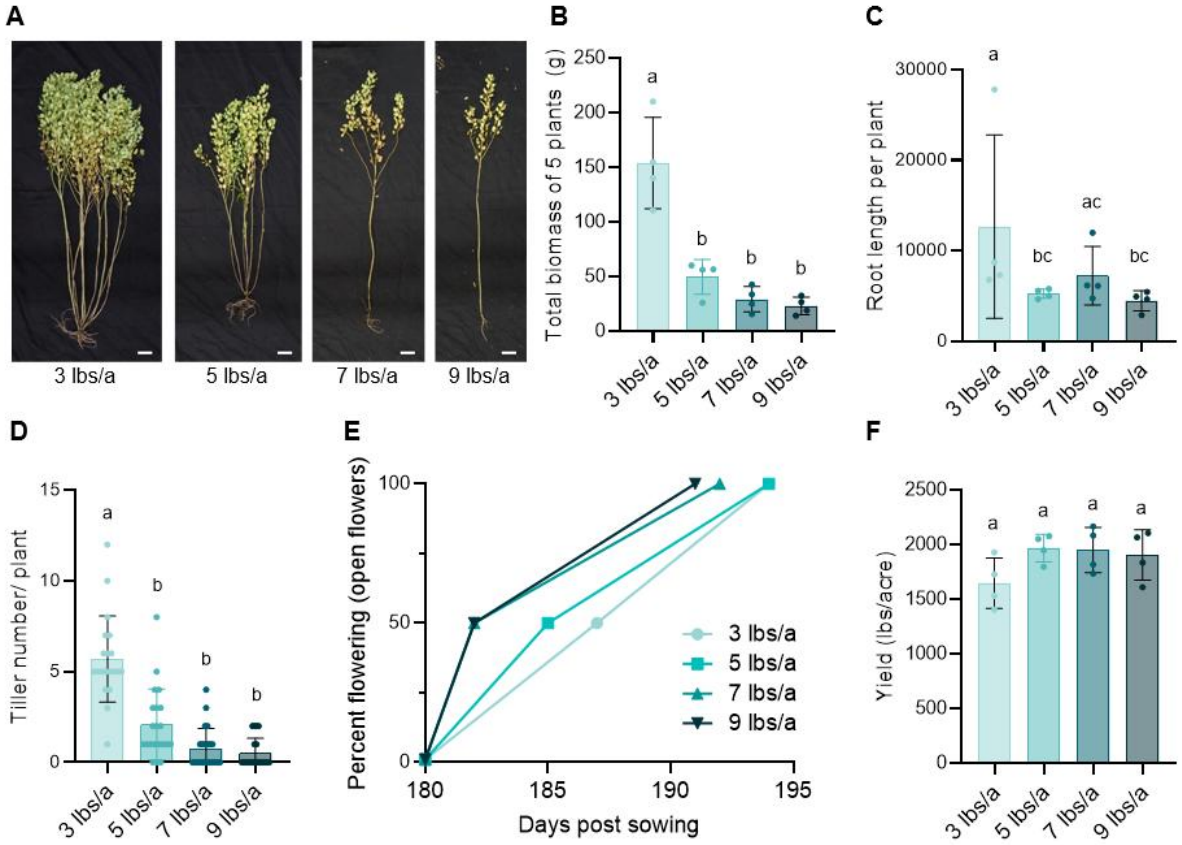

Figure 1. Biomass and yield negatively correlate with seeding density. **(A)** Four plots were sown at 3, 5, 7, and 9 lbs/a. At maturity, 5 plants were harvested from the middle of the plot and imaged. Representative images of individuals from plots are shown. **(B)** Dried biomass of 5 plants. Statistical significance determined by 2-tailed Welch's t-test ($n=4$, $p<0.05$). **(C)** Total root length per plant was determined from soil cores. One core was taken from the middle of each plot. Root length per plant was determined using Rhizovision Explorer and divided by the number of tap roots present in the core. Statistical significance determined by 2-tailed Mann-Whitney test ($n=4$, $p<0.05$) Common letters indicated no significant difference. **(D)** The number of tillers per plant was counted from harvested individuals. Statistical significance determined by 2-tailed Mann-Whitney test. ($n \geq 20$, $p<0.05$). **(E)** Plots were scored for the dates when each reached 50% and 100% flowering. **(F)** Plots were harvested and yield for each plot was determined. Statistical significance determined by 2-tailed Welch's t-test ($n=4$, $p<0.05$).

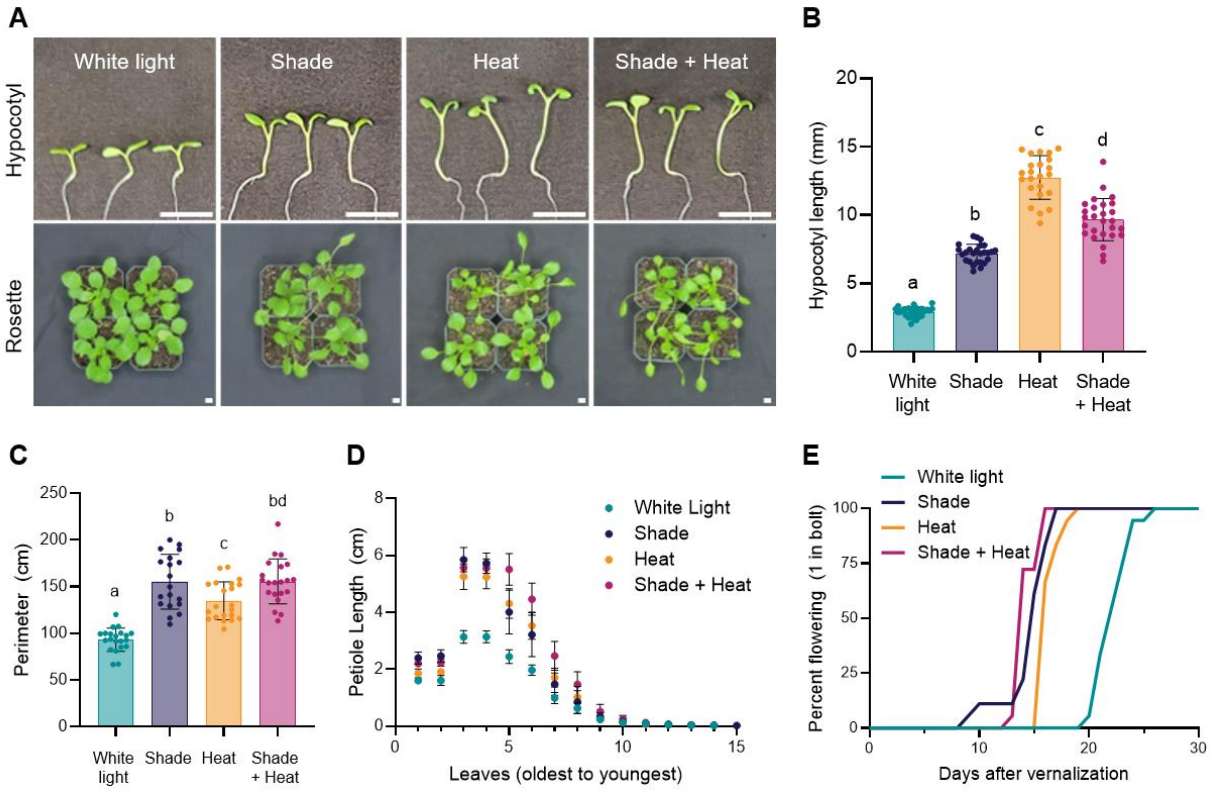

Figure 2. Pennycress increases responses to shade and elevated temperatures. **(A)** Elongation of 5-d-old seedlings grown in white light, shade, heat, and shade + heat. Rosette morphology of plants treated for 6 d with shade, heat, or shade + heat. Scale bar = 1 cm. **(B)** Hypocotyl length of 5-d-old seedings grown in the indicated treatment for 3 d. Statistical significance determined by 2-tailed Welch's t-test ($\pm$ SD, $n \geq 23$, $p < 0.05$). **(C)** Perimeter of 3-week-old rosettes grown in white light, shade, heat, or shade + heat for 14 d. Statistical significance determined by 2-tailed Welch's t-test ($\pm$ SD, $n \geq 19$, $p < 0.05$). **(D)** Petiole length of each leaf of a 17 d-old rosette treated for 7 d. Leaves 1 and 2 are cotyledons (n = 14). **(E)** Number of days till flowering. Plants were considered flowering when the bolt ≥ 1 inch (n= 18).

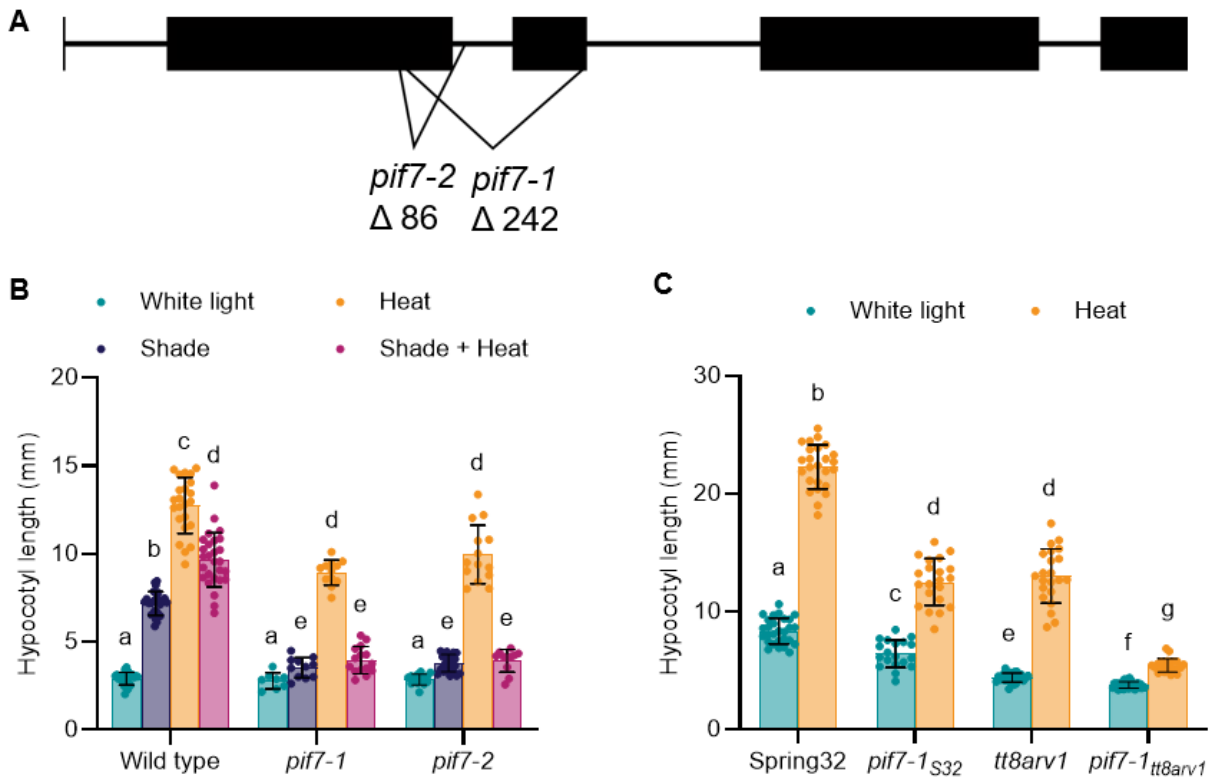

Figure 3. *pif7* has reduced hypocotyl elongation across genetic backgrounds in response to shade and heat. **(A)** PIF7 gene diagram depicting mutations. Exons are black boxes. *pif7-1* and *pif7-2* were generated with CRISPR in the MN106 wild-type background. **(B)** Hypocotyl length of 5 d old seedlings. Seeds were germinated in white light for 2 d, then grown in shade, heat, or shade + heat, for an additional 3 d. Statistical significance determined by 2-tailed Welch's t-test (± SD, $n \geq 8$, $p < 0.05$). Data for wild type is the same from Figure 2B replotted. **(C)** Hypocotyl length of 5 d-old seedlings, germinated in white light for 2 d, then grown in heat for an additional 3 d. Statistical significance determined by 2-tailed Welch's t-test (± SD, $n \geq 19$, $p < 0.05$). Common letters indicated no significant difference.

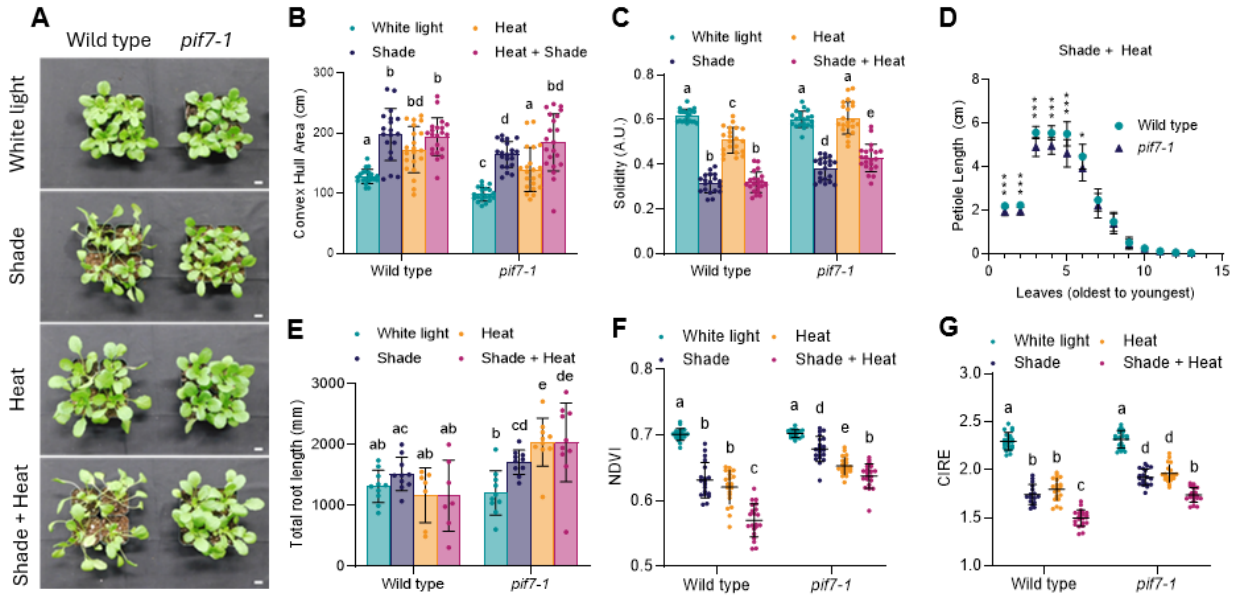

Figure 4. *pif7* attenuates responses to foliar shade and heat throughout vegetative growth. **(A)** Representative plants grown in control conditions for 7 d then for 14 d in treatment conditions and imaged. **(B)** Rosette solidity of plants grown in control conditions for 7 d then for 14 d in treatment conditions. Solidity was determined using the shape analysis function from PlantCV. **(C)** The convex hull area of rosettes was calculated using the shape analysis function from PlantCV. **(D)** Petiole length of each leaf of plants grown in control conditions for 10 d then moved to shade + heat environment for an additional 8 d. Plants were dissected to measure petiole length of each leaf. Leaves are arranged oldest to youngest; cotyledons are leaves 1 and 2. Statistical significance was determined by 2-tailed Welch's t-test (± SD, n = 14, p* < 0.05, p** < 0.01, p*** <0.001). **(E)** Total root length of plants grown on MS plates for 7 d then transferred to turface. Plants were then grown in treatment conditions for 10 d. Roots were washed, scanned, and analyzed with Rhizovision (± SD, n ≥ 7, p < 0.05). **(F)** Seeds were sown in soil and grown in long day control conditions (22 °C, 200 µmol m^{-2} s^{-1}, R:Fr =12) for 7 d. On day 7, conditions were changed to shade (22 °C, 200 µmol m^{-2} s^{-1}, R:Fr = 0.3), heat (28 °C, 200 µmol m^{-2} s^{-1}, R:Fr =12) or shade + heat (28 °C, 200 µmol m^{-2} s^{-1}, R:Fr = 0.3). Elevated temperature and the far-red ratio were maintained only during the day. Normalized Difference Vegetation Index (NDVI) and **(G)** chlorophyll index-red edge (CIRE) were measured in dark adapted plants after 14 d of being grown in the indicated environment. Statistical significance was determined by a 2-tailed Welch's t-test (±SD, n ≥16, p < 0.05). Common letters indicated no significant difference.

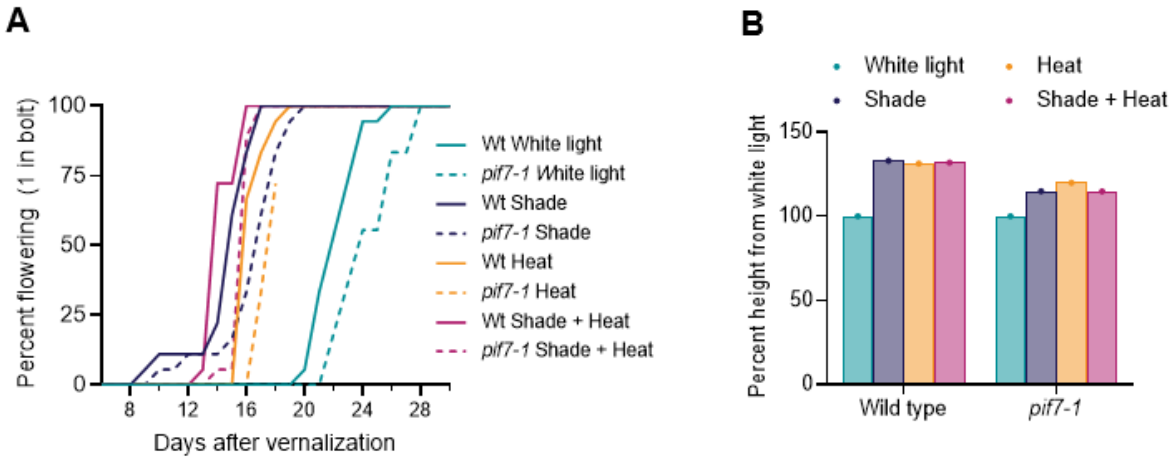

Figure 5. *pif7* attenuates responses to foliar shade and heat through reproductive phases. **(A)** Flowering time of plants grown for 1 week, vernalized for 3 weeks, then moved back to control conditions for 5 d. Plants were then transferred to the indicated treatment condition for and grown for 14 d before returning to control conditions. When bolts reached 1 inch, plants were scored as flowering. (n = 18) **(B)** Plant height was measured at maturity. Height was normalized to height of appropriate genotype to plants grown under white light for the duration of the experiment (n ≥ 16).

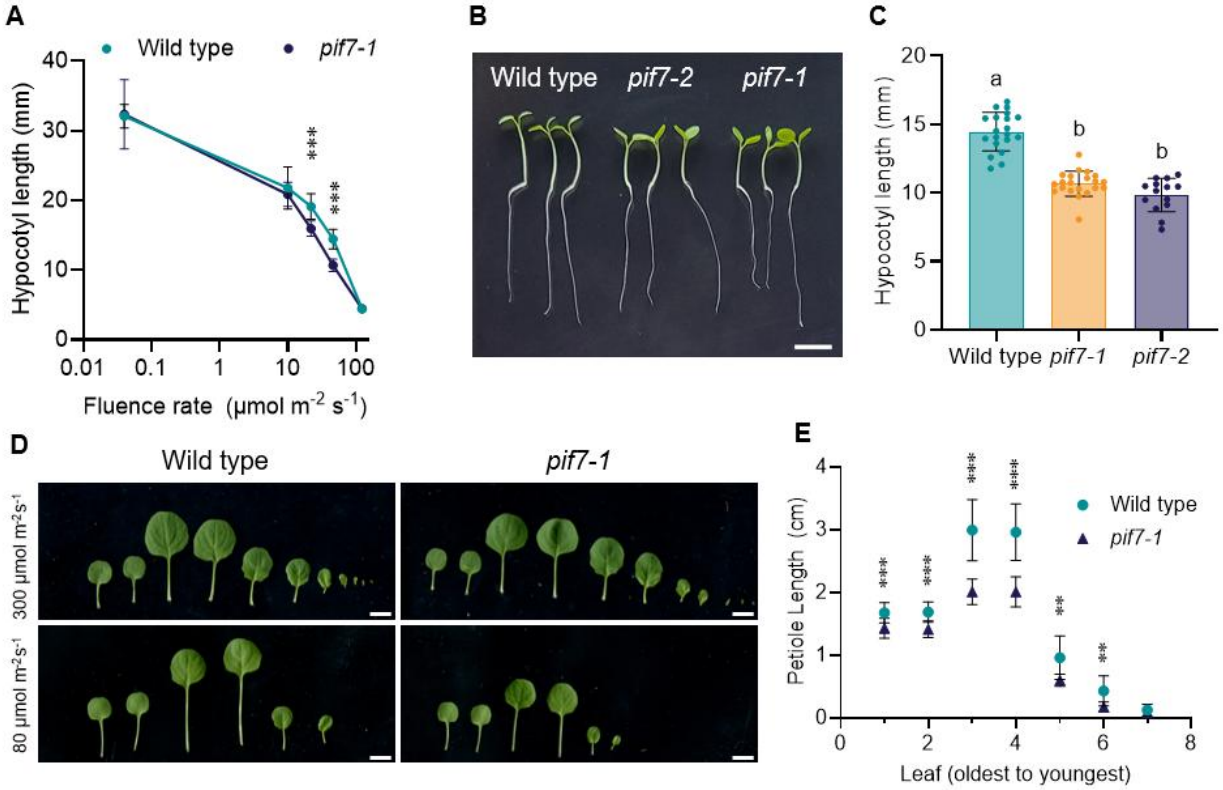

Figure 6. *pif7* has reduced organ elongation in low fluence conditions **(A)** Seedlings were germinated in white light at 120 µmol m^{-2} s^{-1} for 2 d. On day 3, seedlings were grown under various neutral density filters to reduce PAR. Hypocotyls were measured on day 6. Statistical significance was determined by 2-tailed Welch's t-test. (± SD, n ≥ 14, p* < 0.05, p** < 0.01, p*** <0.001) **(B)** Representative hypocotyls at 45 µmol m^{-2} s^{-1}. Scale bar = 5 mm. **(C)** Hypocotyl length of seeding germinated at 120 µmol m^{-2} s^{-1} for 2 d then grown under LEE209 filter to reduce PAR to 45 µmol m^{-2} s^{-1} for an additional 4 d. Statistical significance was determined by 2-tailed Welch's t-test (± SD, n ≥ 14, p < 0.05). Wild type and *pif7-3* data from Figure 5A was used to graph Figure 5C and image for Figure 5B. **(D)** Representative leaves of plants grown under control light and low light conditions. Plants were sown and grown for 1 week at 300 µmol m^{-2} s^{-1}. Half of the plants were moved to 80 µmol m^{-2} s^{-1} of light and grown for an additional week, the other half was kept under control light conditions. On day 15 plants were dissected. Leaves were arranged from oldest to youngest. Scale bar = 1 cm **(E)** Petiole length of each leaf of wild type and *pif7-3* grown at 80 µmol m^{-2} s^{-1}. Statistical significance determined by 2-tailed Welch's t-test (± SD, n ≥ 14, p* < 0.05, p** < 0.01, p*** <0.001). Common letters indicated no significant difference.

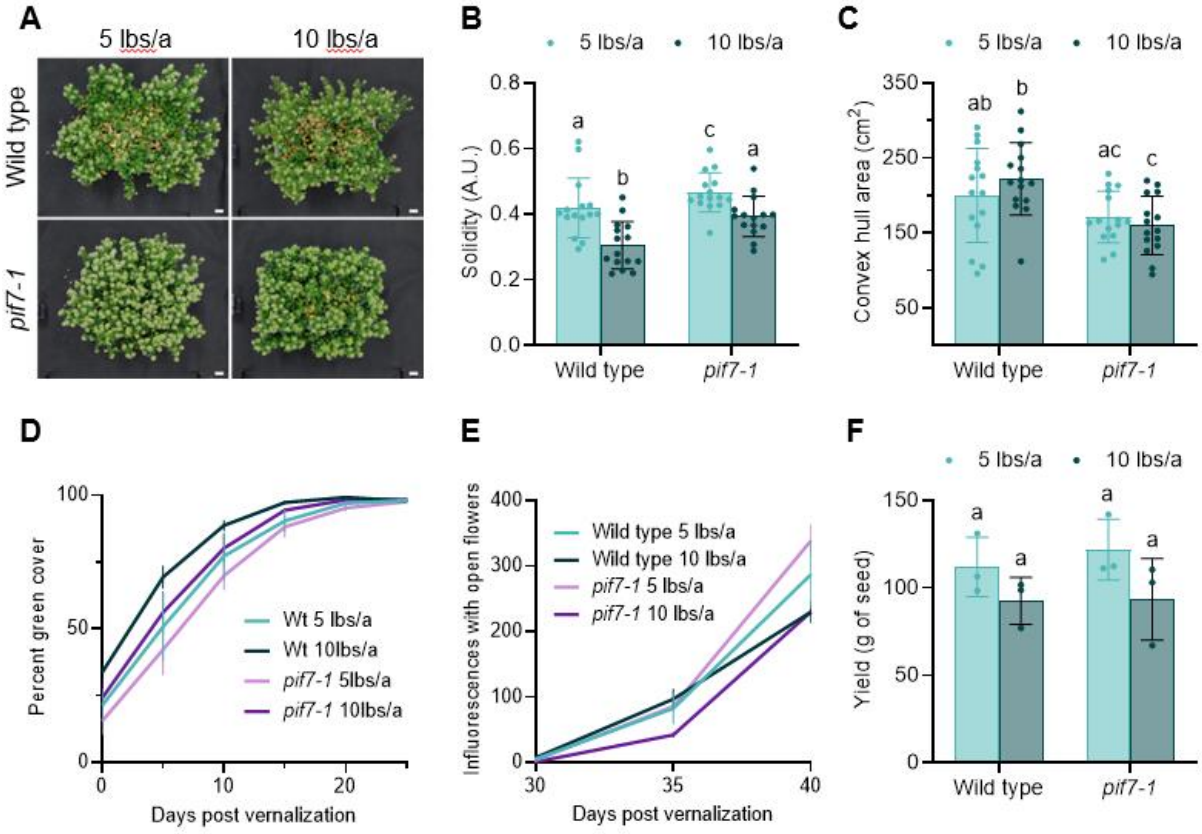

Figure 7. *pif7* attenuates elongation when grown at high density without reducing yield. MN106 and *pif7-1* seeds were sown in 27 L Sterilite containers measuring 59.7 cm x 42.9 cm x 14.9 cm at 5 and 10 lbs/a. The mini fields were grown for 2 weeks, vernalized for 21 d, moved back to standard growing conditions and imaged every 5 d. **(A)** Mini-fields 40 d after vernalization. **(B)** 5 rosettes were pulled at random from each mini field 11 d after vernalization. Solidity and **(C)** Convex hull area was calculated using the morphology function from PlantCV. Statistical significance determined by 2-tailed Mann-Whitney test (±SD, n = 15, $p < 0.05$). **(D)** Percent green coverage within the boundary of the mini-field was calculated from overheard images taken every 5 days post vernalization with PlantCV. **(E)** Inflorescences with open flowers were counted in each mini-field. **(F)** All seeds were harvested for each mini-field to calculate average yield. Statistical significance determined by 2-tailed Mann-Whitney test (±SD, n = 3, $p < 0.05$). Common letters indicated no significant difference.

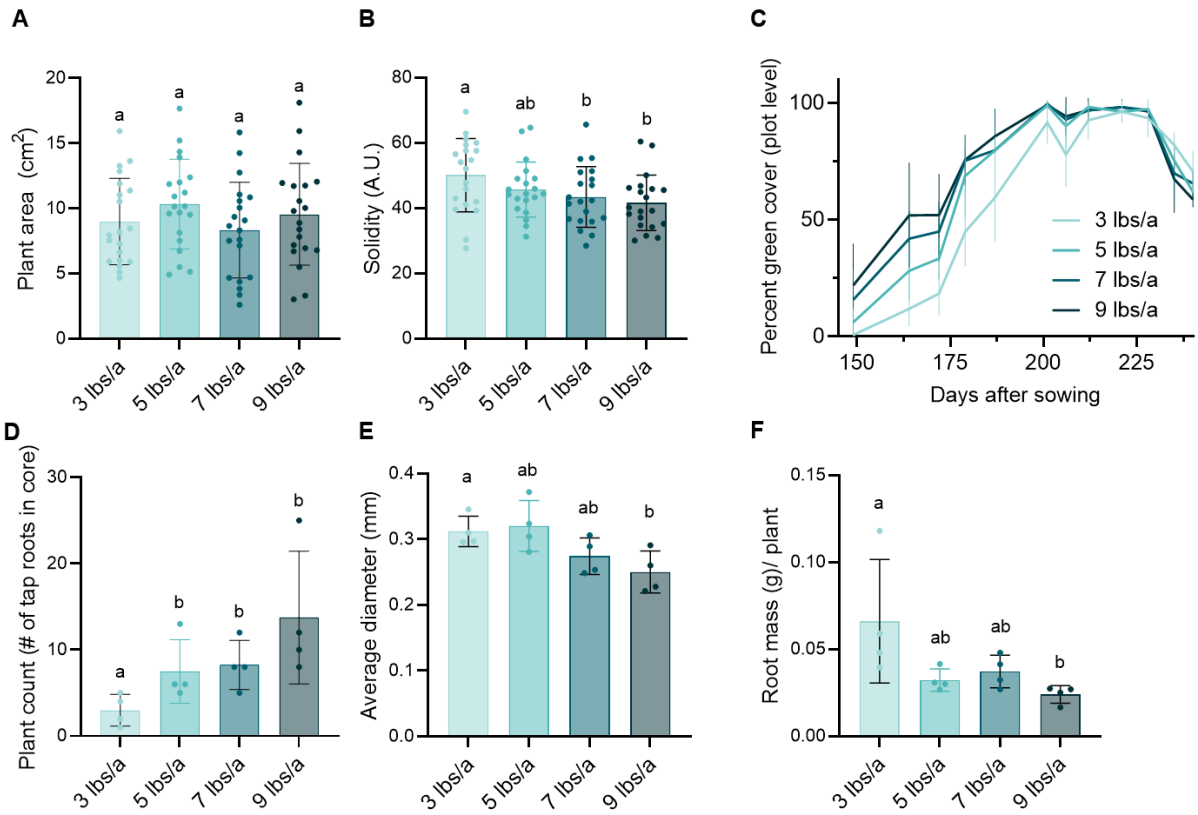

Supplemental Figure 1. Additional measurements from field. Five individuals were removed from each density plot and imaged on 12-04-2023, 64 days after planting. **(A)** Plant area and **(B)** solidity was calculated using the shape analysis function from PlantCV. Statistical significance was determined using 2-tailed Mann-Whitney test (±SD, n = 16, $p < 0.05$). **(C)** Percent green cover of each plot was calculated to estimate plant coverage of soil from drone images. **(D)** Soil cores were taken from the center of each plot. Tap roots from each core were counted providing a number of plants present. Statistical significance was determined using 2-tailed Wilcoxon rank sum test (±SD, n = 4, $p < 0.05$). **(E)** Root traits were measured using Rhizovision. Root diameter of all roots in the core were averaged. Statistical significance was determined using 2-tailed Wilcoxon rank sum test (±SD, n = 4, $p < 0.05$). **(F)** Roots were washed and tried to measure biomass. Total biomass was divided by the number of tap roots in the core to estimate root mass per plant. Statistical significance was determined using 2-tailed Wilcoxon rank sum test (±SD, n = 4, $p < 0.05$).

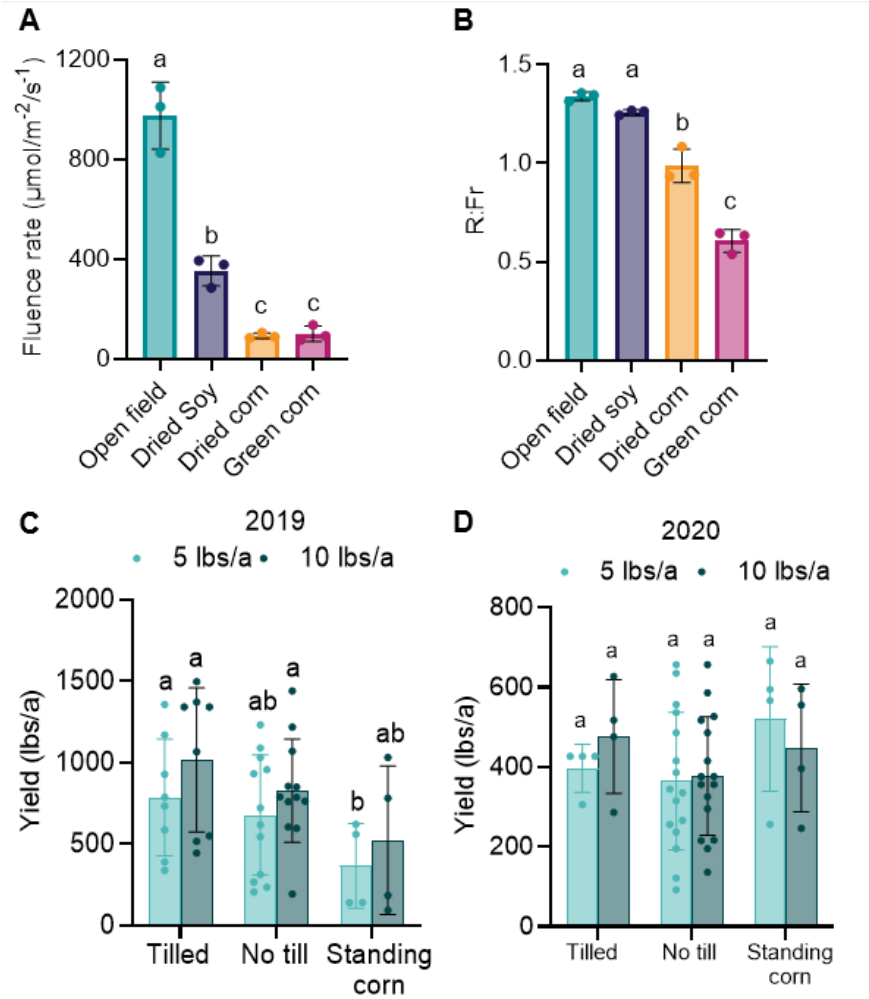

Supplemental Figure 2. Light intensity and quality are altered in interseeded fields and affect yield. **(A)** Light intensity and **(B)** quality were measured on a partly cloudy day on 10-23-2023 between 1- 3 pm with an Li-180. Standing corn measured approximately 9 ft in height. Light readings were taken by walking down a straight line and taking 10- 12 measurements approximately every 10 feet. These measurements were averaged to be 1 repetition. This was repeated in a different location of the same field condition 2 more times for a total of 3 repetitions, accounting for over 30 individual readings. Statistical significance was determined using 2-tailed Welch's t-test (±SD, $n = 3$, $p < 0.05$). **(C)** Yield from plots of pennycress sown in tilled fields, non tilled fields, and standing corn in **(C)** 2019 and **(D)** 2020. Statistical significance was determined using the 2-tailed Mann-Whitney test (±SD, $n \geq 4$, $p < 0.05$). Common letters indicated no significant difference

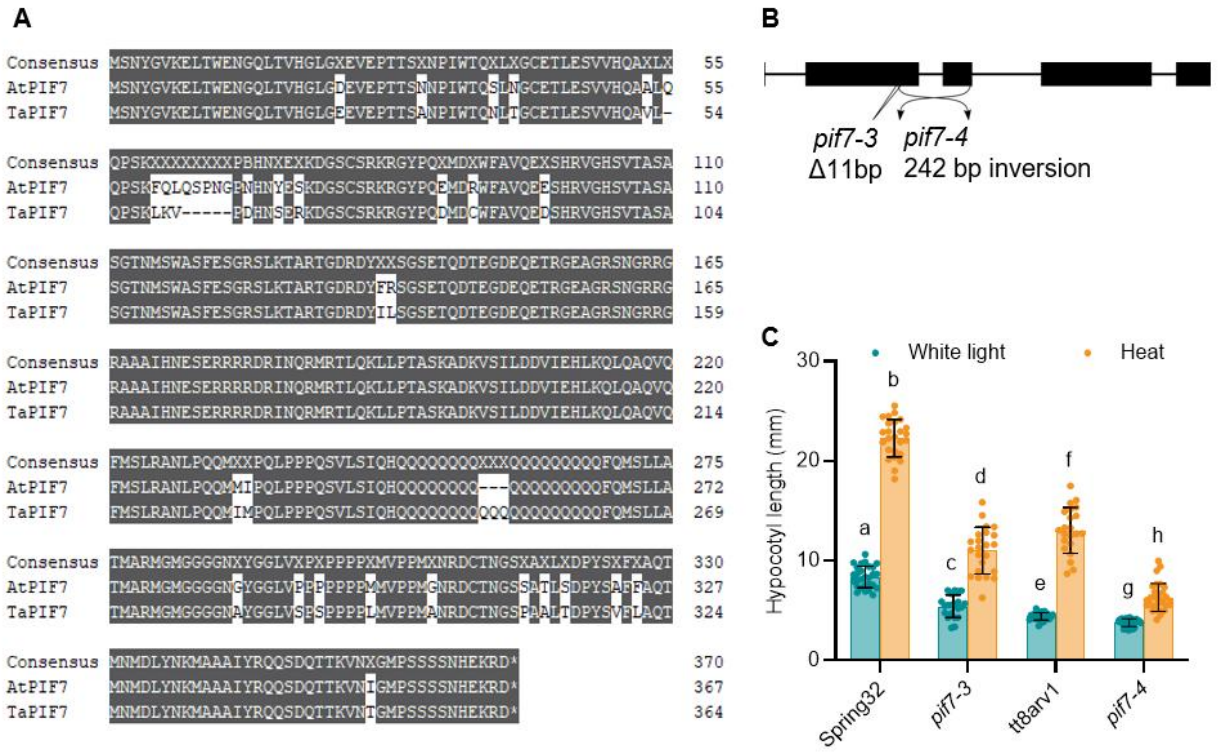

Supplemental Figure 3. (A) *Thlaspi arvese* PIF7 (TaPIF7) is highly similar to *Arabidopsis thaliana* PIF7 (AtPIF7) and *pif7* has reduced elongation in heat. **(A)** Amino acid alignment of pennycress PIF7 (TaPIF7) and Arabidopsis PIF7 (AtPIF7). Agreements with the consensus are highlighted. **(B)** PIF7 gene diagram depicting additional alleles generated by CRISPR-CAS9. Exons are black boxes. *pif7-3,* in the Spring32 genetic background, is a small deletion of 11 bases that results in a frameshift. *pif7-4*, in the *tt8ARV1* background is an inversion of the gene sequence between the gRNA targets. **(C)** Hypocotyl length of 5 d-old seedlings, germinated in white light for 2 d, then grown in heat for an additional 3 d. Statistical significance determined by 2-tailed Welch's t-test ($\pm$ SD, $n \geq 21$, $p < 0.05$). Common letters indicated no significant difference.

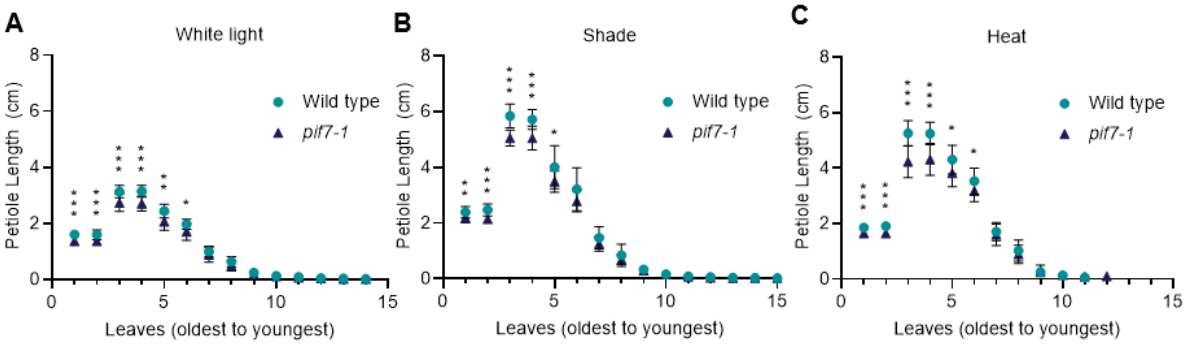

Supplemental Figure 4. *pif7-1* has reduced responses to environmental conditions Petiole length was measured for each leaf of a rosette grown in **(A)** white light, **(B)** shade, and **(C)** heat. Plants were initially grown in control conditions for 10 d before moving to treatment conditions for 8 d before dissection. Leaves are arranged oldest to youngest; cotyledons are leaves 1 and 2. Statistical significance was determined by 2-tailed Welch's t-test (± SD, n = 14, p* < 0.05, p** < 0.01, p*** <0.001).

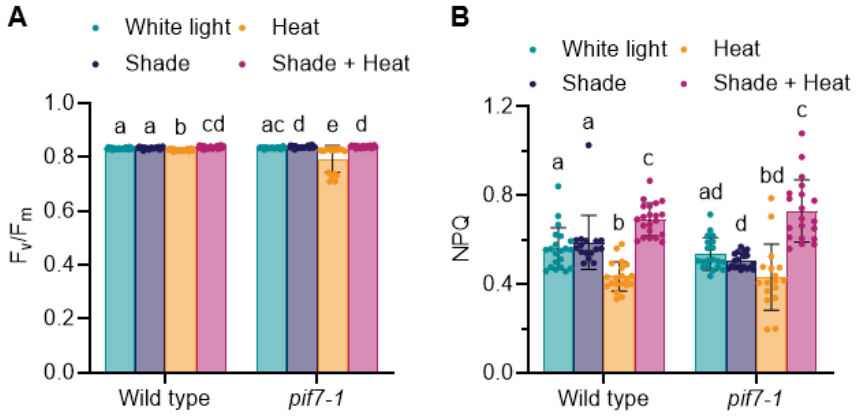

Supplemental Figure 5. Chlorophyll fluorescence of plants grown in shade and heat. Seeds were sown in soil and grown in long day control conditions (22 °C, 200 µmol m^{-2} s^{-1}, R:Fr =12) for 7 d. On day 7, conditions were changed to shade (22 °C, 200 µmol m^{-2} s^{-1}, R:Fr = 0.3), heat (28 °C, 200 µmol m^{-2} s^{-1}, R:Fr =12) or shade + heat (28 °C, 200 µmol m^{-2} s^{-1}, R:Fr = 0.3). Elevated temperature and the far-red ratio were maintained only during the day. **(A)** F_v/F_m and **(B)** NPQ were measured in dark adapted plants after 14 d of being grown in the indicated environment. Statistical significance was determined by a 2-tailed Welch's t-test (±SD, n ≥16, $p < 0.05$). Common letters indicated no significant difference.

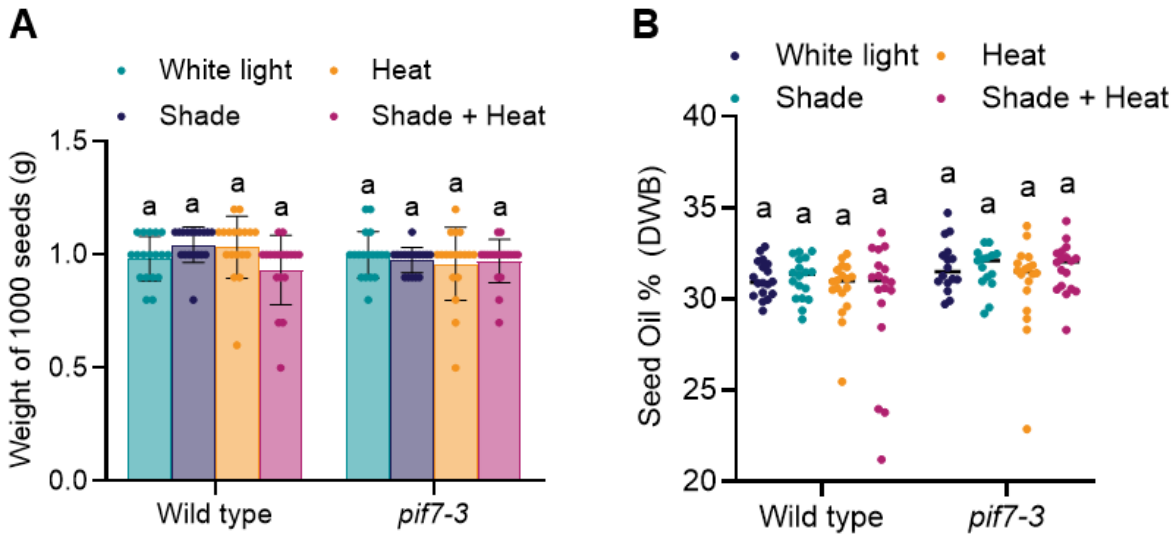

Supplemental Figure 6. *pif7* does not alter seed weight and oil content. were measured. (A) Plants at the rosette state were transferred to the indicated condition for 14 d after vernalization then moved back to control conditions to mature. Statistical significance was determined by 2-tailed Welch's t-test (± SD, n ≥ 17, $p < 0.05$). (B) 1000 seeds from each plant were weighed. Statistical significance was determined by 2-tailed Mann-Whitney test (± SD, n ≥ 17, $p < 0.05$). (C) Seed oil percentage on a dry weight basis (DWB) was measured in seeds. Statistical significance was determined by 2-tailed Mann-Whitney test (± SD, n ≥ 15, $p < 0.05$).

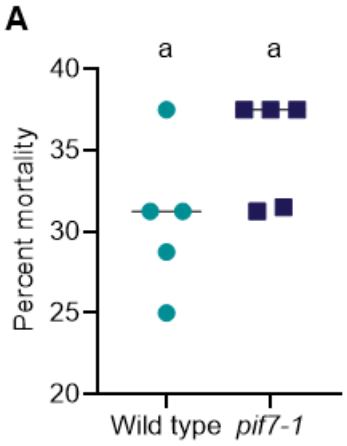

Supplemental Figure 7. *pif7* maintains freezing tolerance. Plants were grown for 2 weeks, vernalized for 3 weeks at 4 °C, then subjected to freezing treatment down to -10 °C. Plants were returned to the greenhouse and evaluated for survival after a 10 d recovery period. 16 plants of each genotype were tested for freezing tolerance in 5 independent tests.Statistical significance was determined by 2-tailed Mann-Whitney test (± SD, $n \geq 5$, $p < 0.05$). Common letters indicated no significant difference.

References

Arief, M.A.A. et al., 2023. Chlorophyll fluorescence imaging for early detection of drought and heat stress in strawberry plants. *Plants*, 12(6), p.1387.

Assefa, Y. et al., 2018. Analysis of long term study indicates both agronomic optimal plant density and increase maize yield per plant contributed to yield gain. *Scientific reports*, 8(1), p.4937.

Balcerowicz, M., 2020. PHYTOCHROME-INTERACTING FACTORS at the interface of light and temperature signalling. *Physiologia plantarum*, 169(3), pp.347–356.

Bauer, D. et al., 2004. Constitutive photomorphogenesis 1 and multiple photoreceptors control degradation of phytochrome interacting factor 3, a transcription factor required for light signaling in Arabidopsis. *The Plant cell*, 16(6), pp.1433–1445.

Bishop, L. & Nelson, K.A., 2019. Field pennycress seeding date and corn herbicide management effects on corn, pennycress, and soybean production. *Agronomy journal*, 111(1), pp.257–263.

Burko, Y. et al., 2022. PIF7 is a master regulator of thermomorphogenesis in shade. *Nature communications*, 13(1), p.4942.

Cao, Y. et al., 2022. Leaf angle: a target of genetic improvement in cereal crops tailored for high-density planting. *Plant biotechnology journal*, 20(3), pp.426–436.

Casal, J.J. & Balasubramanian, S., 2019. Thermomorphogenesis. *Annual review of plant biology*, 70(1), pp.321–346.

Casal, J.J. & Fankhauser, C., 2023. Shade avoidance in the context of climate change. *Plant physiology*, 191(3), pp.1475–1491.

Cerdán, P.D. & Chory, J., 2003. Regulation of flowering time by light quality. *Nature*, 423(6942), pp.881–885.

Clack, T., Mathews, S. & Sharrock, R.A., 1994. The phytochrome apoprotein family in Arabidopsis is encoded by five genes: the sequences and expression of PHYD and PHYE. *Plant molecular biology*, 25(3), pp.413–427.

Cubins, J.A. et al., 2019. Management of pennycress as a winter annual cash cover crop. A review. *Agronomy for sustainable development*, 39(5), pp.1–11.

Delker, C., Quint, M. & Wigge, P.A., 2022. Recent advances in understanding thermomorphogenesis signaling. *Current opinion in plant biology*, 68(102231), p.102231.

Dorn, K.M. et al., 2015. A draft genome of field pennycress (Thlaspi arvense) provides tools for the domestication of a new winter biofuel crop. *DNA research: an international journal for*

rapid publication of reports on genes and genomes, 22(2), pp.121–131.

Dose, H.L. et al., 2017. Early planting dates maximize winter annual field pennycress (Thlaspi arvense L.) yield and oil content. *Industrial crops and products*, 97, pp.477–483.

Duvick, D.N., 2005. The Contribution of Breeding to Yield Advances in maize (Zea mays L.). In *Advances in Agronomy*. Advances in agronomy. Elsevier, pp. 83–145.

Elli, E.F. et al., 2023. Maize leaf angle genetic gain is slowing down in the last decades. *Crop science*, 63(6), pp.3520–3533.

Fan, J. et al., 2013. A life cycle assessment of pennycress (Thlaspi arvense L.) -derived jet fuel and diesel. *Biomass and Bioenergy*, 55, p.87.

Fernández, V. et al., 2016. Photoperiodic and thermosensory pathways interact through CONSTANS to promote flowering at high temperature under short days. *The Plant journal: for cell and molecular biology*, 86(5), pp.426–440.

Fiorucci, A.-S. et al., 2020. PHYTOCHROME INTERACTING FACTOR 7 is important for early responses to elevated temperature in Arabidopsis seedlings. *The New phytologist*, 226(1), pp.50–58.

Franklin, K.A., 2008. Shade avoidance. *The new phytologist*, 179(4), pp.930–944.

Franklin, K.A. & Whitelam, G.C., 2005. Phytochromes and shade-avoidance responses in plants. *Annals of botany*, 96(2), pp.169–175.

Galvão, V.C. et al., 2019. PIF transcription factors link a neighbor threat cue to accelerated reproduction in Arabidopsis. *Nature communications*, 10(1), p.4005.

Gehan, M.A. et al., 2017. PlantCV v2: Image analysis software for high-throughput plant phenotyping. *PeerJ*, 5, p.e4088.

van Gelderen, K. et al., 2018. Far-red light detection in the shoot regulates lateral root development through the HY5 transcription factor. *The plant cell*, 30(1), pp.101–116.

Ghosh, D., Mohapatra, S. & Dogra, V., 2023. Improving photosynthetic efficiency by modulating non-photochemical quenching. *Trends in plant science*, 28(3), pp.264–266.

Gray, S.B. & Brady, S.M., 2016. Plant developmental responses to climate change. *Developmental biology*, 419(1), pp.64–77.

Griffiths, M. et al., 2022. Optimisation of root traits to provide enhanced ecosystem services in agricultural systems: A focus on cover crops. *Plant, cell & environment*, 45(3), pp.751–770.

Jung, J.-H. et al., 2016. Phytochromes function as thermosensors in Arabidopsis. *Science*, 354(6314), pp.886–889.

Kami, C. et al., 2010. Light-regulated plant growth and development. *Current topics in developmental biology*, 91, pp.29–66.

Kidokoro, S. et al., 2009. The phytochrome-interacting factor PIF7 negatively regulates DREB1 expression under circadian control in Arabidopsis. *Plant physiology*, 151(4), pp.2046–2057.

Kim, R.J.A. et al., 2024. Photobody formation spatially segregates two opposing phytochrome B signaling actions to titrate plant environmental responses. *bioRxiv : the preprint server for biology*. Available at: http://dx.doi.org/10.1101/2023.11.12.566724.

Lee, C.-M. & Thomashow, M.F., 2012. Photoperiodic regulation of the C-repeat binding factor (CBF) cold acclimation pathway and freezing tolerance in Arabidopsis thaliana. *Proceedings of the National Academy of Sciences of the United States of America*, 109(37), pp.15054–15059.

Legris, M. et al., 2016. Phytochrome B integrates light and temperature signals in *Arabidopsis*. *Science*, 354(6314), pp.897–900.

Legris, M., Ince, Y.Ç. & Fankhauser, C., 2019. Molecular mechanisms underlying phytochrome-controlled morphogenesis in plants. *Nature communications*, 10(1), pp.1–15.

Li, L. et al., 2012. Linking photoreceptor excitation to changes in plant architecture. *Genes & development*, 26(8), pp.785–790.

Li, S. et al., 2021. Estimating the contribution of plant traits to light partitioning in simultaneous maize/soybean intercropping. *Journal of experimental botany*, 72(10), pp.3630–3646.

Liu, Y., Jafari, F. & Wang, H., 2021. Integration of light and hormone signaling pathways in the regulation of plant shade avoidance syndrome. *aBIOTECH*, 2(2), pp.131–145.

Lorrain, S. et al., 2008. Phytochrome-mediated inhibition of shade avoidance involves degradation of growth-promoting bHLH transcription factors. *The Plant journal: for cell and molecular biology*, 53(2), pp.312–323.

Lu, J. et al., 2023. Row ratio increasing improved light distribution, photosynthetic characteristics, and yield of peanut in the maize and peanut strip intercropping system. *Frontiers in plant science*, 14, p.1135580.

Maxwell, K. & Johnson, G.N., 2000. Chlorophyll fluorescence—a practical guide. *Journal of experimental botany*, 51(345), pp.659–668.

McGinn, M. et al., 2019. Molecular tools enabling pennycress (Thlaspi arvense) as a model plant and oilseed cash cover crop. *Plant biotechnology journal*, 17(4), pp.776–788.

Mohammed, Y.A. et al., 2020. Establishing winter annual cover crops by interseeding into Maize and Soybean. *Agronomy journal*, 112(2), pp.719–732.

Moser, B.R., 2012. Biodiesel from alternative oilseed feedstocks: camelina and field pennycress.

Biofuels, 3(2), pp.193–209.

Moser, B.R., Evangelista, R.L. & Isbell, T.A., 2016. Preparation and Fuel Properties of Field Pennycress (Thlaspi arvense) Seed Oil Ethyl Esters and Blends with Ultralow-Sulfur Diesel Fuel. *Energy & fuels: an American Chemical Society journal*, 30(1), pp.473–479.

Murchie, E.H. & Lawson, T., 2013. Chlorophyll fluorescence analysis: a guide to good practice and understanding some new applications. *Journal of experimental botany*, 64(13), pp.3983–3998.

Nozue, K. et al., 2007. Rhythmic growth explained by coincidence between internal and external cues. *Nature*, 448(7151), pp.358–361.

Nunn, A. et al., 2022. Chromosome-level Thlaspi arvense genome provides new tools for translational research and for a newly domesticated cash cover crop of the cooler climates. *Plant biotechnology journal*, 20(5), pp.944–963.

Oravec, M.W. & Greenham, K., 2022. The adaptive nature of the plant circadian clock in natural environments. *Plant physiology*, 190(2), pp.968–980.

Pantazopoulou, C.K., Bongers, F.J. & Pierik, R., 2021. Reducing shade avoidance can improve Arabidopsis canopy performance against competitors. *Plant, cell & environment*, 44(4), pp.1130–1141.

Park, E. et al., 2012. Phytochrome B inhibits binding of phytochrome-interacting factors to their target promoters. *The Plant journal: for cell and molecular biology*, 72(4), pp.537–546.

Park, E., Kim, Y. & Choi, G., 2018. Phytochrome B Requires PIF Degradation and Sequestration to Induce Light Responses across a Wide Range of Light Conditions. *The Plant cell*, 30(6), pp.1277–1292.

Park, J., Bae, S. & Kim, J.-S., 2015. Cas-Designer: a web-based tool for choice of CRISPR-Cas9 target sites. *Bioinformatics* , 31(24), pp.4014–4016.

Patel, S. et al., 2021. Interseeded pennycress and camelina yield and influence on row crops. *Agronomy journal*, 113(3), pp.2629–2647.

Paulišić, S. et al., 2021. Adjustment of the PIF7-HFR1 transcriptional module activity controls plant shade adaptation. *The EMBO journal*, 40(1), p.e104273.

Pham, V.N., Kathare, P.K. & Huq, E., 2018. Phytochromes and Phytochrome Interacting Factors. *Plant physiology*, 176(2), pp.1025–1038.

Ranganathan, J. et al., 2018. How to Sustainably Feed 10 Billion People by 2050, in 21 Charts. Available at: https://www.wri.org/insights/how-sustainably-feed-10-billion-people-2050-21-charts [Accessed November 14, 2024].

Raza, A. et al., 2020. Agro-techniques for lodging stress management in maize-soybean

intercropping system-A review. *Plants*, 9(11), p.1592.

Rockwell, N.C., Su, Y.-S. & Lagarias, J.C., 2006. Phytochrome structure and signaling mechanisms. *Annual review of plant biology*, 57, pp.837–858.

Roig-Villanova, I. & Martínez-García, J.F., 2016. Plant Responses to Vegetation Proximity: A Whole Life Avoiding Shade. *Frontiers in plant science*, 7, p.236.

Romero-Montepaone, S. et al., 2020. Shade avoidance responses become more aggressive in warm environments. *Plant, cell & environment*, 43(7), pp.1625–1636.

Rosado, D. et al., 2022. WRKY transcription factors and ethylene signaling modify root growth during the shade-avoidance response. *Plant physiology*, 188(2), pp.1294–1311.

Salisbury, F.J. et al., 2007. Phytochrome coordinates Arabidopsis shoot and root development: Phytochrome coordinates development. *The Plant journal: for cell and molecular biology*, 50(3), pp.429–438.

Schiml, S., Fauser, F. & Puchta, H., 2016. Repair of adjacent single-strand breaks is often accompanied by the formation of tandem sequence duplications in plant genomes. *Proceedings of the National Academy of Sciences of the United States of America*, 113(26), pp.7266–7271.

Schmitt, J., Dudley, S.A. & Pigliucci, M., 1999. Manipulative Approaches to Testing Adaptive Plasticity: Phytochrome-Mediated Shade-Avoidance Responses in Plants. *The American naturalist*, 154(S1), pp.S43–S54.

Seethepalli, A. et al., 2021. RhizoVision Explorer: open-source software for root image analysis and measurement standardization. *AoB plants*, 13(6), p.lab056.

Sessa, G. et al., 2018. Multiple pathways in the control of the shade avoidance response. *Plants*, 7(4), p.102.

Sharrock, R.A., 2008. The phytochrome red/far-red photoreceptor superfamily. *Genome biology*, 9(8), p.230.

Sharrock, R.A. & Quail, P.H., 1989. Novel phytochrome sequences in Arabidopsis thaliana: structure, evolution, and differential expression of a plant regulatory photoreceptor family. *Genes & development*, 3(11), pp.1745–1757.

Smith, H., 1982. Light quality, photoperception, and plant strategy. *Annual review of plant physiology*, 33(1), pp.481–518.

Stamford, J.D. et al., 2023. Development of an accurate low cost NDVI imaging system for assessing plant health. *Plant methods*, 19(1), p.9.

Tang, Y.-J. & Liesche, J., 2017. The molecular mechanism of shade avoidance in crops – How data from Arabidopsis can help to identify targets for increasing yield and biomass

production. *Journal of integrative agriculture*, 16(6), pp.1244–1255.

Trupkin, S.A. et al., 2014. Phytochrome B nuclear bodies respond to the low red to far-red ratio and to the reduced irradiance of canopy shade in Arabidopsis. *Plant physiology*, 165(4), pp.1698–1708.

Us Epa, O., 2021. Climate Change Indicators: Seasonal Temperature. Available at: https://www.epa.gov/climate-indicators/climate-change-indicators-seasonal-temperature [Accessed November 21, 2024].

Wille, W. et al., 2017. Reducing shade avoidance responses in a cereal crop. *AoB plants*, 9(5), p.lx039.

de Wit, M. et al., 2018. Changes in resource partitioning between and within organs support growth adjustment to neighbor proximity in Brassicaceae seedlings. *Proceedings of the National Academy of Sciences of the United States of America*, 115(42), pp.E9953–E9961.

de Wit, M. et al., 2016. Integration of Phytochrome and Cryptochrome Signals Determines Plant Growth during Competition for Light. *Current biology: CB*, 26(24), pp.3320–3326.

Xu, M., Hu, T. & Poethig, R.S., 2021. Low light intensity delays vegetative phase change. *Plant physiology*, 187(3), pp.1177–1188.

York, L.M., Nord, E.A. & Lynch, J.P., 2013. Integration of root phenes for soil resource acquisition. *Frontiers in plant science*, 4, p.355.